ARDHI UNIVERSITY

ASSESSMENT OF DISPARITY DUE TO USE OF DEMS OF DIFFERENT RESOLUTIONS IN COMPUTATION OF RESIDUAL TERRAIN EFFECT (RTE'S).

SWAI, HAPPINESS F

BSc. Geomatics

Dissertation

Ardhi University, Dar es Salaam

July, 2023

ASSESSMENT OF DISPARITY DUE TO USE OF DEMS OF DIFFERENT RESOLUTIONS IN COMPUTATION OF RESIDUAL TERRAIN EFFECT (RTE'S).

By

SWAI, HAPPINESS F

"A Dissertation Submitted to the Department of Geospatial Sciences and Technology in Partially Fulfilment of the Requirements for the Award of Science in Geomatics (BSc. GM) of Ardhi University"

CERTIFICATION

The undersigned certify that she has read and hereby recommends for acceptance by the Ardhi University a dissertation titled **"Assessment of Disparity Due to Use of DEMs of Different Resolutions in Computation of Residual Terrain Effect (RTE's)."**, in fulfilment of the requirements for the award of degree of Bachelor of Science in Geomatics of the Ardhi University.

…….……

Ms. Regina V. Peter

(Main Supervisor)

Date……

DECLARATION AND COPYRIGHT

I, *Swai, Happiness F*, hereby declare that this thesis is my own original work and to the best of my knowledge it has not been presented to any other University or Institution of higher learning for a degree or similar award.

…….....

Swai, Happiness F

22785/T.2019

(candidate)

ACKNOWLEDGEMENT

First and foremost, praises and thanks to the God Almighty, for His showers of blessings throughout my study at ARU and completion of my research successfully.

I would like to express my sincere gratitude to my research supervisor, Ms. Regina Valerian Peter and Mr. Humphrey Busega for giving me the support throughout this research. Your comments, criticism, hard questions and encouragement have given me the courage and confidence to complete this research successfully. Also, I would like to thank Dr. Ulotu, P. E, Mr.Kwimbere and Mr.Mutaraguza for their dynamism, vision, sincerity and motivation that have deeply inspired me to fall in love with geomatic field.

I would also like to acknowledge all the academic and non-academic staff of the Department of Geospatial Sciences and Technology (DGST) for the direct and indirect support during my studies. Also, my thanks go to all the people who supported me to complete the research work directly or indirectly.

I am extremely grateful to my parents for their love, prayers, caring and sacrifices for educating and preparing me for my future to be a better person. Also, I express my sincere gratitude to my sisters Victoria and Neema and my brother Danniel for their support and valuable prayers.

I would like also to acknowledge my closest and special person in my life George Cyprian for his support and his endless love.

I would like to thank my research colleagues Salma Kodi, Protas Siriwa, Gabriel Nyaradani, Chove Lupyana and Abdul-Rahim for the discussions, encouragement and support.

Swai, Happiness F

July,2023.

DEDICATION.

To my father Swai, Francis and mother Lyimo, Conjesta. Also, to my beloved sisters; Victoria Swai and my brothers; Daniel Swai Your presence always makes me motivated and determined.

ABSTRACT

Research aims at assessing the disparity that arises when using digital elevation models (DEMs) of varying resolutions in the computation of residual terrain effects (RTE). RTE is due to the topographic masses relative to a level surface through the point, or relative to some other approximation to the terrain. To investigate this disparity, DEMs of different resolutions were obtained and compared in terms of their accuracy and ability to capture fine-scale terrain features. The study utilized a high-resolution DEM as the reference dataset and compared it with lower-resolution DEMs generated by downscaling techniques.

The statical results of the computed RTEs shows that MERIT DEM has mean of -14.493 and STD of 32.381, TANDEM-X has mean of -14.995 and STD of 32.381, FABDEM has mean of -16.474 and STD of 4.894 and ALOSv1-2 DEM has mean of -12.514 and STD of 25.588. The results showed that using lower-resolution DEMs led to a loss of fine-scale terrain details, resulting in an underestimation of RTE.

For validation results difference of RTEs between MERIT DEM and SRTM2gravity has mean of 14.204 and STD of 32.836, difference of RTEs between TANDEM-X and SRTM2gravity has mean of 14.705 and STD of 32.830, difference of RTEs between FABDEM and SRTM2gravity has mean of -3.754 and STD of 7.287 and the difference of RTEs between ALOSv1-2 DEM and SRTM2gravity has mean of 4.171 and STD of 17.323. This means FABDEM and SRTM2gravity compute the same RTE since their differences in RTEs is small in terms of mean and STD

Based on these findings, it is crucial to consider the resolution of the DEM when computing RTE. Higher-resolution DEMs should be used to accurately capture fine-scale terrain features and minimize the disparity in RTE computation. This study highlights the importance of selecting an appropriate DEM resolution for accurate assessment and modelling of residual terrain effects.

Keywords: 1'×1' Residual Terrain Effects (RTE), constant density, MERIT DEM, TANDEM-X, FABDEM, ALOSv1-2 DEM, sparse point gravity data, Tanzania

Table of Contents

List of Figures

List of Tables

LIST OF ABBREVIATIONS

ALOSv2-1	Advanced Land Observing Satellite DEM version 2 at 1 arc second resolution
AOI	Area of Interest
CHAMP	Challenging Mini-satellite Payload
DEM	Digital Elevation Model
DTM	Digital Terrain Model
EGM08	Earth Gravity Model 2008
EGM96	Earth Gravity Model 1996
FABDEM	Forest And Buildings Removed Copernicus DEM
FORTRAN	Formula Translation, a computer programming language
GDEM	Global Digital Elevation Model
GGM	Global Gravitational Model
GMT	Generic Mapping Tool
GOCE	Gravity field and steady state Ocean Circulation Explorer
GRACE	Gravity Recovery And Climate Experiment
GRACE-FO	Gravity Recovery And Climate Experiment Follow-On
Graflab	Gravity Field Laboratory
Gravsoft	Denmark-KMS precise geoid model determination computer package
GRS80	Geodetic Reference System of 1980
GUI	Graphical User Interface
HC	Harmonic Corrections
LITHO1.0	An updated crust and lithospheric model of the Earth at $1° \times 1°$ resolution

MA	Mean Average
MATLAB	Matrix Laboratory
MERIT	Multi-Error-Removed-Terrain
mGal	milli gals
MSL	Mean Sea Level
NASA	National Aeronautics and Space Administration
NI	Numerical Integration
R-C-R	Remove-Compute-Restore Method
r-c-r	remove-compute-restore technique
RMS	Root Mean Square
RTE	Residual Terrain Effects
RTM	Residual Terrain Model
SH	Spherical Harmonics
STD	Standard Deviation
TANDEM-X	TerraSAR-X Add-oN for Digital Elevation Model
TC	Terrain Correction
TGF	Terrain Gravity Field software
WGS84	World Geodetic System 198

CHAPTER ONE

INTRODUCTION

1.1 BACKGROUND.

Precise Modelling of the Earth's gravity field is a key task of physical geodesy, with different applications such as determination of the figure and size of the earth, reduction of Geomatics and geodetic measurements, determination of physical heights and the study of mass distribution within the Earth (Torge & Muller, 2012). In the process of gravimetric modeling, precise terrestrial gravity data is required and must be evenly distributed over the AOI. This is not the case in most of the developing countries like Tanzania, whose gravity data coverage is sparse and mostly found in areas with exploration activities such as mining while leaving big gaps in game reserves and national parks (Ulotu, 2016). Due to this challenge several actions have been taken in densification of gravity in areas which lack gravity information. Figure 1.1 below shows the distribution of gravity data in Tanzania.

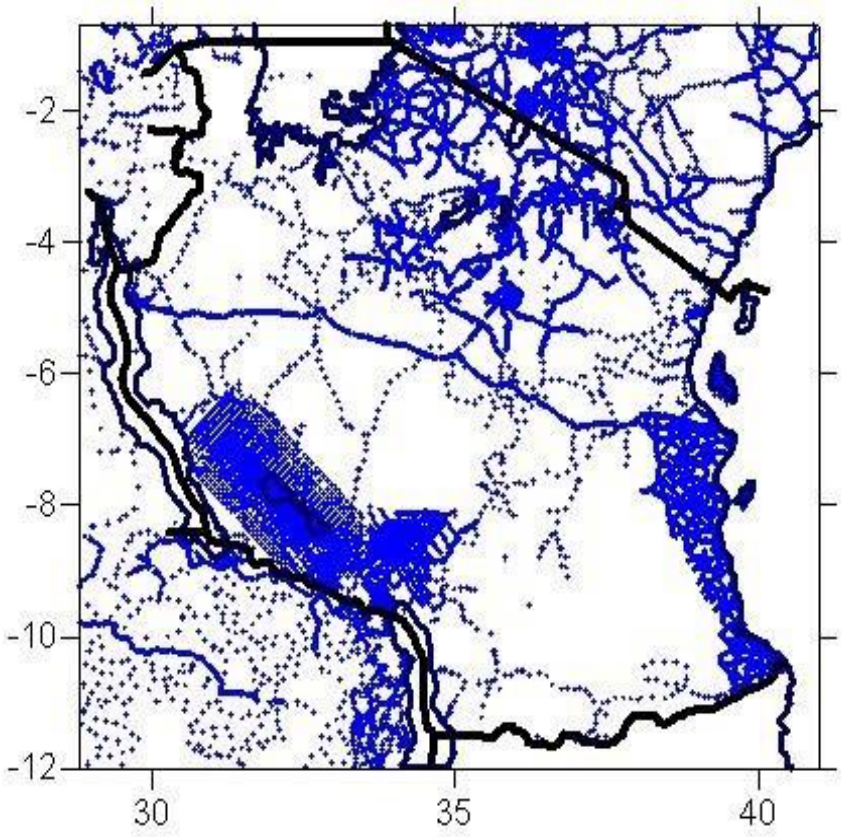

Figure 1.1: Map showing distribution of gravity in Tanzania

The classical stokes formula of geoid determination require that the value of gravity to be known on a reference surface and no masses to be above this reference surface (Heiskanen & Moritz, 1967). Example of this reference is a geoid which can defined as an equipotential surface to the Earth's gravity field that coincides with the mean sea level in least squares however, most of these surfaces are located inside the earth's surface that is to say they contain masses above them sense (Vanicek & Krakiswky, 1986).

To ensure that the gravity information is well distributed across the AOI, we need to do gravity modeling. Before undertaking gravity prediction, the terrestrial gravity is smoothed to remove its erratic nature. Erratic nature is the variation in Earth's gravity field caused by irregular topography and subsurface structures, it's so call erratic because it's not easily predictable and can result in significant differences from idealizes global average gravity field so must be removed or compensated. The long wavelength components are mainly computed from the global gravimetric models (GGMs) and the short wavelengths components are computed from accurate representation of the earth's topography presented in Digital Elevation Models (DEM). Most often, the residual terrain modeling technique (Forsberg, 1984) is used in computation of residual terrain effects (RTE) which yields the short wavelength components. In computations of RTE the knowledge of topographic mass distribution and crustal density is vital in ensuring good results. Gravity reductions serve a tool for geoid determination in geodesy, interpolation/ extrapolation of the gravity and the investigation of the Earth's crust in geophysics and geology (Heiskanen &Mortiz, 1967). By definition gravity reduction is the process of determining gravity on the geoid or inside the land masses from the surface gravity (Hofmann-Wellenhof & Moritz, 2005).

The earth's gravity field can be divided into three components in the spectral domain, i.e., short, medium and long wavelength components. The topography of the earth is the rich source of the high frequencies of the earth's gravity field on land and as a result a high-resolution DEM/DTM can be used to compute these high frequencies through different topographic mass models and methods e.g., Simple and Complete Bouguer plates (planar 11or spherical), Isostatic reduction schemes, Residual Terrain Effect (RTE) etc. For example, due to the displacement from the earth's surface, the aerial gravity observation misses the very high frequency component of gravity.

The low frequency component of gravity is due to the large masses beneath the terrain mainly below the Mean Sea Level (MSL) (Heiskanen & Moritz,1967). The low frequencies (long-wave component of gravity) approximate the actual gravity on the surface of the earth because they lack the details represented by the terrain. The earth's gravity field determined by the dedicated satellite missions (CHAMP, GRACE, GRACE-FO) contains the low frequency component of gravity but GOCE goes further to medium frequencies which are derived from Airborne. See all the components of gravity; high, medium and low frequencies of the earth's gravity field and their sources as shown in the Figure 1.2 below.

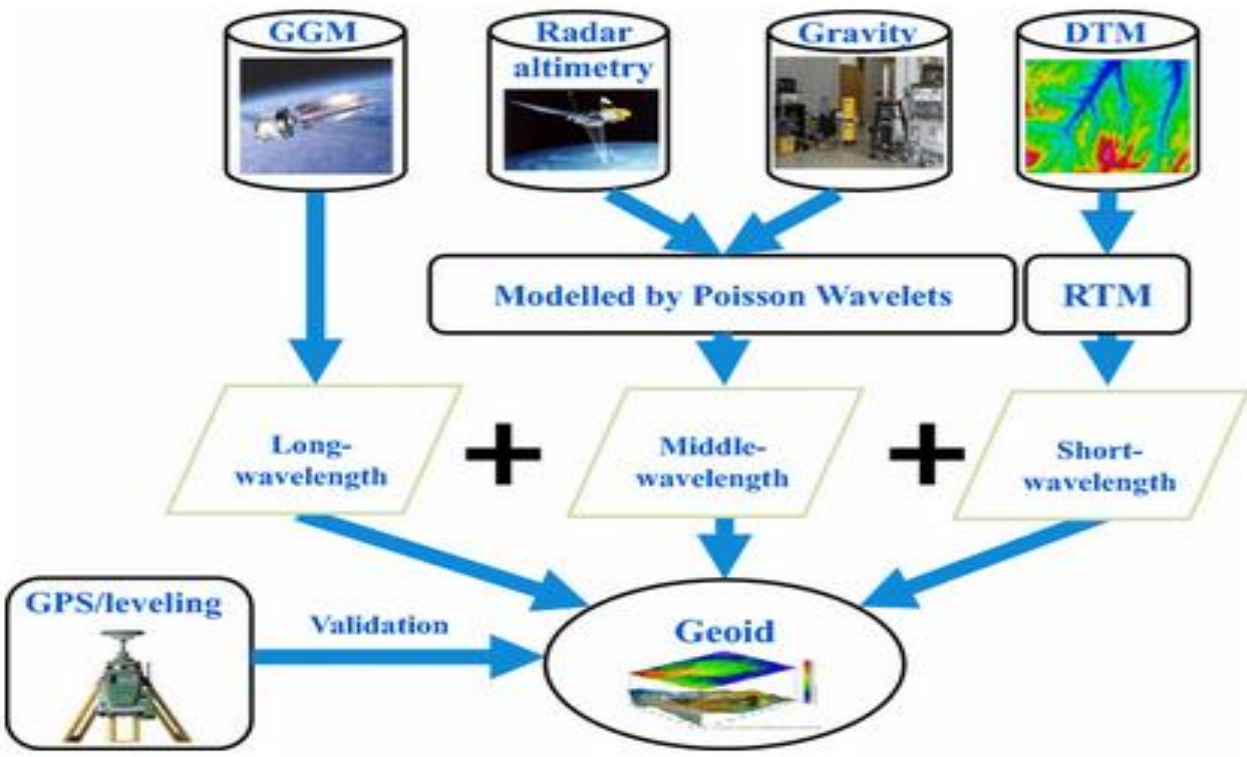

Figure 1.2: Source and spectral components of the earth gravity field

Short wavelength spectral content of gravity is usually due to presence of topography (terrain effect). In geodesy, terrain effect can be either total terrain effect or residual terrain effect (RTE). Total terrain effect at a point is due to all the topographic masses above the geoid while residual 1terrain effect is due to the topographic masses relative to a level surface through the point, or relative to some other approximation to the terrain. Theoretically, Residual terrain model (RTM) is used to compute residual terrain effect. In RTM, a smooth mean elevation surface also called reference surface is chosen, and masses above this surface are removed to fill up valleys below.

RTM was introduced by (Forsberg, 1984) for RCR approaches, in this technique topographic irregularities relative to a smooth mean elevation surface, with resolution comparable to that of the used GGM are computationally removed. This involves the removal of long and short wavelengths components of the gravity. The long wavelength components are mainly computed from the global gravimetric models (GGMs) and short wavelengths components are computed from accurate representation of the earth's topography presented in Digital Elevation Models (DEM). Most often, the residual terrain modeling technique (Forsberg, 1984) is used in computation of residual terrain effects (RTE) which yields the short wavelength components. In computations of RTE the knowledge of topographic mass distribution and crustal density is vital in ensuring good results. RTE is due to topographic masses relative to a level surface through a point or relative to some approximation to the terrain.

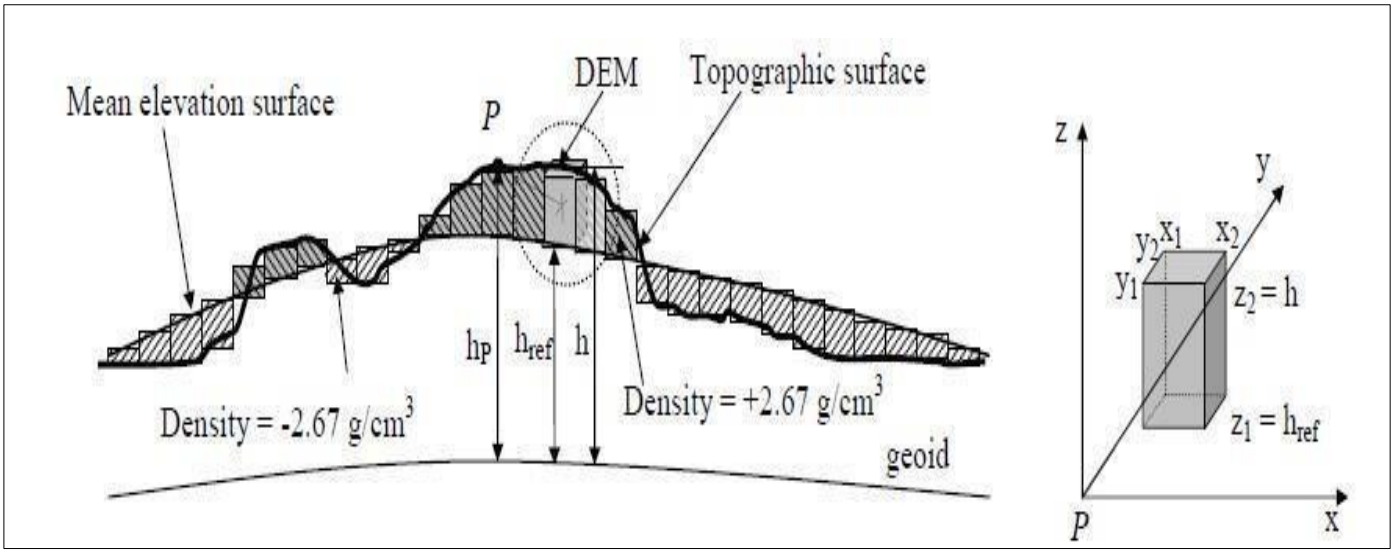

Figure 1.3: Residual Terrain model (Mai, 2012)

RTEs can be computed either by using DEMs or topographic potential models. A Digital Elevation Model (DEM) is a digital representation of the Earth's surface topography. It is a three-dimensional grid of elevation values that provides information about the height or elevation of the terrain at various points across the Earth's surface. DEMs are essential tools in various fields, such as geography, cartography, geology, geodesy, environmental modeling, and engineering.

Many researches have been carried on over several years for different purpose for computing RTEs using DEMs depending on the interest of the individual researcher. Some researchers compute RTEs using constant density and others based on varying density (LITHO1.0). This constant density value ($2670 kg/m^3$) was first computed by Harness (1891) using five values of density of surface rocks published from 1811 to 1882 (Hinze, 2003). Globally several authors went on using this constant density value in computations of RTE (Forsberg, 1984; Omang & Forsberg, 2000; Tziavos et al., 2010; Hirt, 2010; 2 Bucha et al.,2016; Peter, 2018; Rexer et al., 2018; Hirt et al., 2019).

Locally (Tanzania mainland) (Busega & Kimboi, 2018) uses DEM with 6' resolution to compute $1' \times 1'$ RTE grid with the mean of -0.62 and STD of 17.83, (Layda, 2020) compute RTE from ALOSv2 DEM using both constant and varying densities RTE of LITHO1.0 crustal density model has RMS of 23.812mGal and of constant density has RMS of 23.974mGal and (Kabala, 2022) compute $1' \times 1'$ RTE from MERIT DEM (3 arcsec) using different computation packages with the mean and STD of -0.368 and 3.270mGals respectively.

All these researchers only compute RTEs of the specific DEM either based on constant density or varying density (LITHO1.0) but didn't show the disparity due to use of DEMs. Means didn't show if DEMs compute the same RTE over the AOI. Therefore, this study aims at assessing the disparity due to use of DEMs of different resolution.

1.2 STATEMENT OF RESEARCH PROBLEM.

Precise terrestrial gravity data is required in the process of gravimetric modelling, and must be evenly distributed over the area of interest (AOI). This is not the case in most of the developing countries like Tanzania, whose gravity data coverage is sparse and mostly found in areas with exploration activities such as mining while leaving big gaps in game reserves and national parks. Due to this challenge several actions have been taken in densification of gravity in areas which lack gravity information. Thorough computation of RTE gravity data will be obtained easily through prediction. The

completion of this result will aid to show the disparity of RTEs due to use of DEMs of different resolutions.

1.3 OBJECTIVES.

1.3. 1 Main objective

The main objective of this research is assessment of disparity of RTEs due to use of different resolution DEM.

1.3.2 Specific objectives

- Generating $1' \times 1'$ computation points.
- Generating forward masses.
- Computation of Residual Terrain Effect (RTE) from DEMs of different resolutions.

1.4 RESEARCH QUESTIONS.

- Does the resolution of DEMs matters in computation of RTE?
- Which DEM provide the best result of RTE?

1.5 SIGNIFICANCE OF THE RESEARCH.

The research will increase confidence on users of the DEM on different applications like terrain and gravity prediction, flooding and fluid transportation.

1.6 BENEFICIARIES.

This research will benefit geoscientists especially geodesists and Geomatician in;

i. In gravity smoothing and prediction.
ii. Improving gravity prediction through R-C-R approach iii.
iii. To densify the sparse gravity to a suitable density and distribution.
iv. In creating a geodetic boundary surface such as geoid.
v. In determination of gravity gradients.

1.7 SCOPE AND LIMITATIONS.

Scope of this research is to assess the disparity arise when DEMs of different resolutions are used in computation of Residual Terrain Effects (RTE's) using TGF package at 1 ' x 1 ' resolution in Tanzania. RTE's can either be computed from DEMs or from topographic potential models but this research is limited to use DEMs to compute RTE's. The research will be carried on the area which is limited

within 4°N to 15°S latitude and 26°E to 44°E longitude on which Tanzania is within the boundaries, (1°N to 12S °latitude and 29°E to 41°E longitude). Figure 1.4 below shows study area.

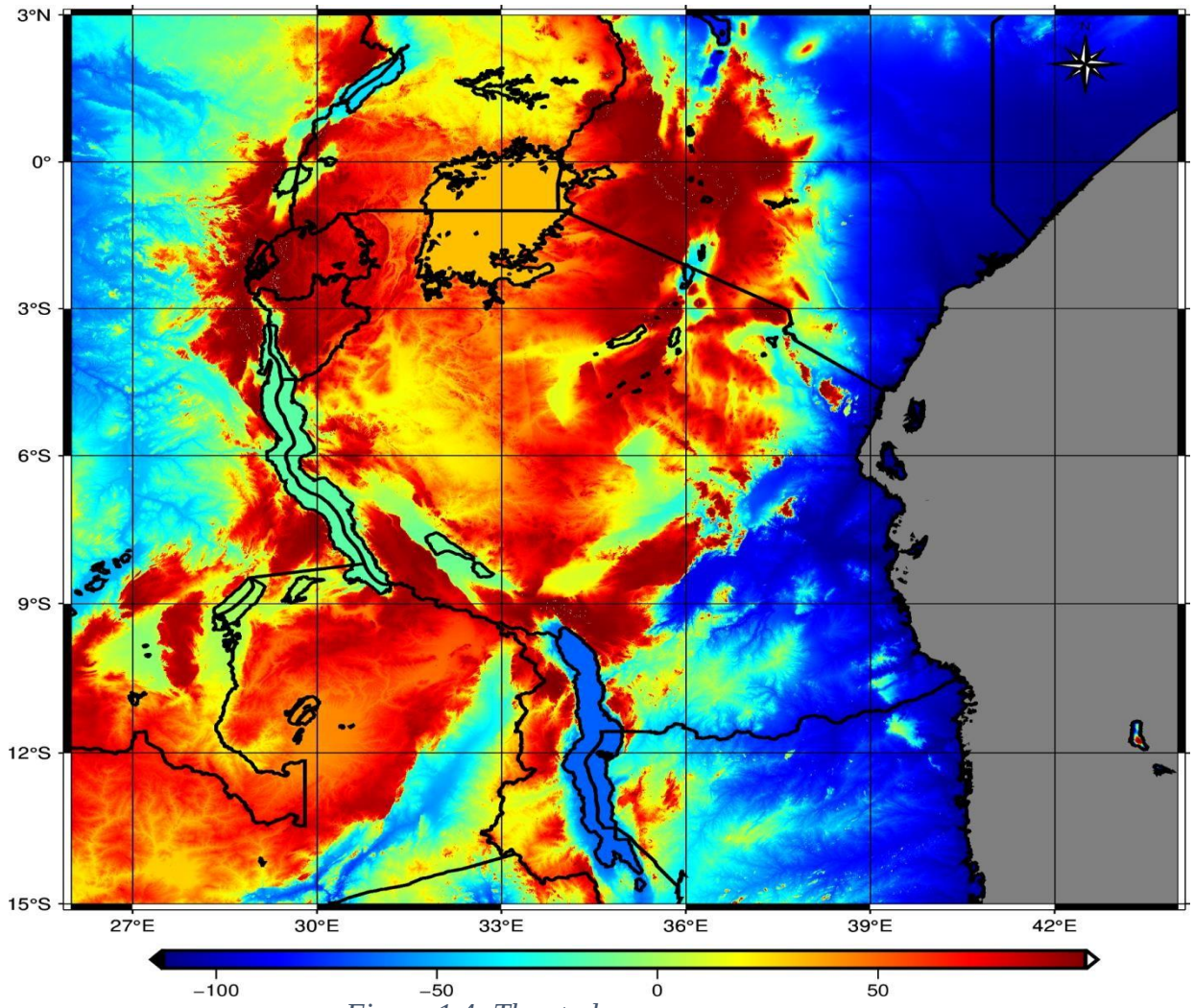

Figure 1.4: The study area

1.8 RESEARCH OUTLINE

This dissertation is divided into five chapters, where;

Chapter one introduces the research by providing the background of the research, what other researchers have done and what gap is left behind. Then, it discusses on the research problem and how it will be tackled.

In chapter two, a thorough literature review about overview of earth's gravity field, the spectral components of earth's gravity field and the overview of the geodetic gravity field modelling programs is described.

In chapter three, the methodology on how the research problem was tackled is discussed. Data used and software's used in this dissertation are also presented.

In chapter four, the results based on the methodology described are presented. Different tables and maps are presented for the easy of interpretation the data. Then, the results are discussed.

Lastly, Chapter five draws out the conclusion and places recommendations on the future research

CHAPTER TWO

LITERATURE REVIEW

2.1 OVERVIEW OF EARTH GRAVITY FIELD

Earth's gravitational field is an interdisciplinary application of Newton's law of universal gravitation and gravitational field strength concept. Newton demonstrated that the force of gravity, F_g, between two objects is attractive, directly proportional to the product of their masses, m_1 and m_2, and inversely proportional to the distance, d, between them squared. Where G is universal Gravitational constant ($6.67 \times 10^{-11} Nm^2/kg^2$).

$$F_g = G\frac{m_1 m_2}{d^2} \quad \text{...} \quad (2.1)$$

Newton's formula can be applied to very large bodies like the Earth and moon system or even the Earth and sun system because of the substantial masses of the objects and the distances between them.

Since gravity is an attractive force and bodies near the Earth's surface fall to Earth, g is also referred to as the average acceleration due to gravity. At sea level, the standard acceleration of gravity is $9.80665\ m/s^2$. Latitude, altitude, and local geology can impact the value of g. Local variations in values of g are called anomalies. They are measured in units of milli Galileo, mGal, which has an acceleration value of about 1×10^{-6} g or $1 \times 10^{-5}\ m/s^2$. To study and understand this non-uniformity, scientists use sophisticated technologies such as satellite gravimetry and gravity models. The resulting gravity models show variations in gravitational acceleration, often referred to as gravitational anomalies, which occur due to differences in the density and distribution of materials within the Earth's interior. For example, areas with denser rocks or minerals exhibit slightly stronger gravitational attraction, while regions with less dense materials exhibit weaker attraction.

One essential reference surface related to the Earth's gravity field is the geoid, which represents the surface of constant gravitational potential energy and closely corresponds to mean sea level. It serves as a crucial reference for measuring elevations and heights on Earth, essential for various applications such as surveying, cartography, and satellite navigation systems like GPS.

The maps provided are color coded to indicate areas with higher (red), or lower (blue), than expected values of g. With imaging from GRACE satellites and a shaded relief map, students can establish and confirm patterns among Earth's gravitational acceleration, topography, and geology.

By examining gravitational anomalies compared to relief features, students quickly identify and confirm the relationship Newton established between mass and gravitational field strength.

2.2 SPECTRAL COMPONENTS OF THE EARTH'S GRAVITY FIELD

The earth's gravity field can be divided into three components in the spectral domain, i.e., high, medium and low frequency components. The topography of the earth is the rich source of the high frequencies of the earth's gravity field on land and as a result a high-resolution DEM/DTM can be used to compute these high frequencies through different topographic mass models and methods e.g., Simple and Complete Bouguer plates (planar or spherical), Isostatic reduction schemes, Residual Terrain Effect (RTE) etc. The high frequency of the earth's gravity field is due to erratic uppermost layer of the earth.

Moving away from the earth's surface, the high frequencies of the earth's gravity field grow weaker and for this reason the details of the figure of the earth also are not sensed. For example, due to the displacement from the earth's surface, the aerial gravity observation misses the very high frequency component of gravity. The low frequency component of gravity is due to the large masses beneath the terrain mainly below the Mean Sea Level (MSL) (Heiskanen & Moritz, 1967). The low frequencies are an approximation of the actual gravity on the surface of the earth because they lack the details represented by the terrain. The earth's gravity field determined by the dedicated satellite missions (CHAMP, GRACE and GRACE-FO) contains the low frequency component of gravity but GOCE goes further to medium frequencies. Mostly, when gravity is needed, it should have all the components; high, medium and low frequencies of the earth's gravity field.

2.2.1 Overview of Gravimetric Terrain Reduction Methods

By definition gravity reduction is the process of determining gravity on the geoid or inside the land masses from the surface gravity (Hofmann-Wellenhof & Moritz, 2005). When conducting gravity reduction, there are two steps involved. The first is removing or compressing all the topographic masses above the geoid and the second is downward continuation of the surface gravity point to the geoid (ibid).

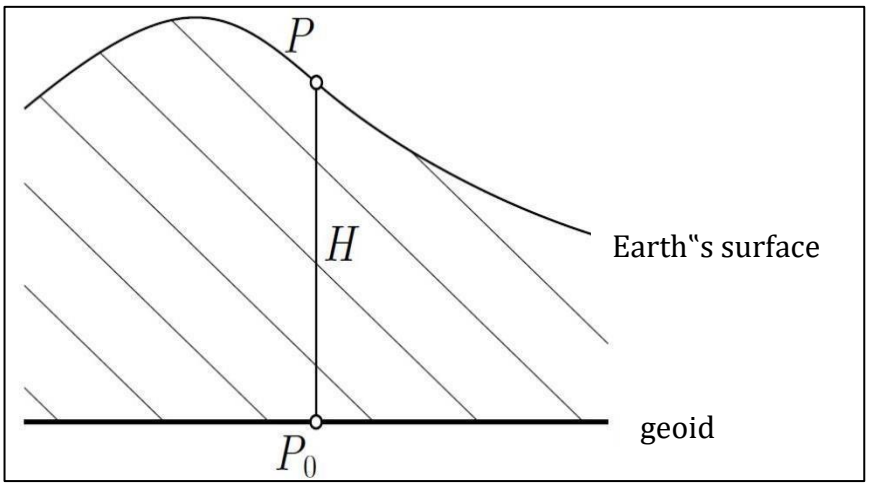

Figure 2.1: Demonstration of gravity reduction (Hofmann-Wellenhof & Moritz, 2005)

In the process of removing topographic masses, several approaches have been used based on how they treat topographic masses. These processes are referred to as gravimetric terrain reduction which can be defined as the process of removing or compressing topographic masses above the reference surface (geoid).

Gravimetric terrain reduction is widely applied in most of the of physical geodesy activities such as;

i. In gravity smoothing and prediction.
ii. In creating a geodetic boundary surface such as geoid.
iii. In determination of gravity gradients.

There are numerous methods involved in gravimetric terrain reduction; some of them are described below.

A. The Bouguer Reduction

This method basically removes all the topographic masses above the reference surface such as the geoid (Hofmann-Wellenhof & Moritz, 2005). It was derived from the formula of computing the gravitational potential of a point due to a cylinder of density, thickness *H* and radius *a* as shown in Figure 2.2 (Saburi et al., 2010).

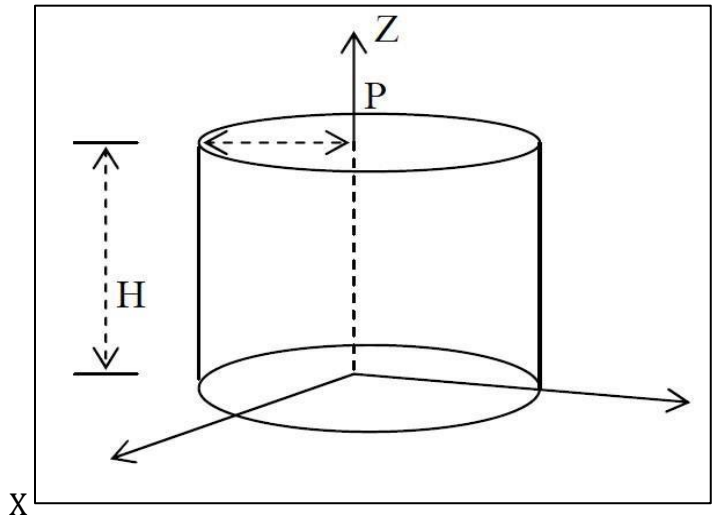

Figure 2.2: Potential of a cylinder

It assumes that at each terrain point *P*, the area around it to be completely flat with an infinite radius and thickness, h_p which equals to the elevation of the computation point *P* to the given datum as shown in Figure (2.3).

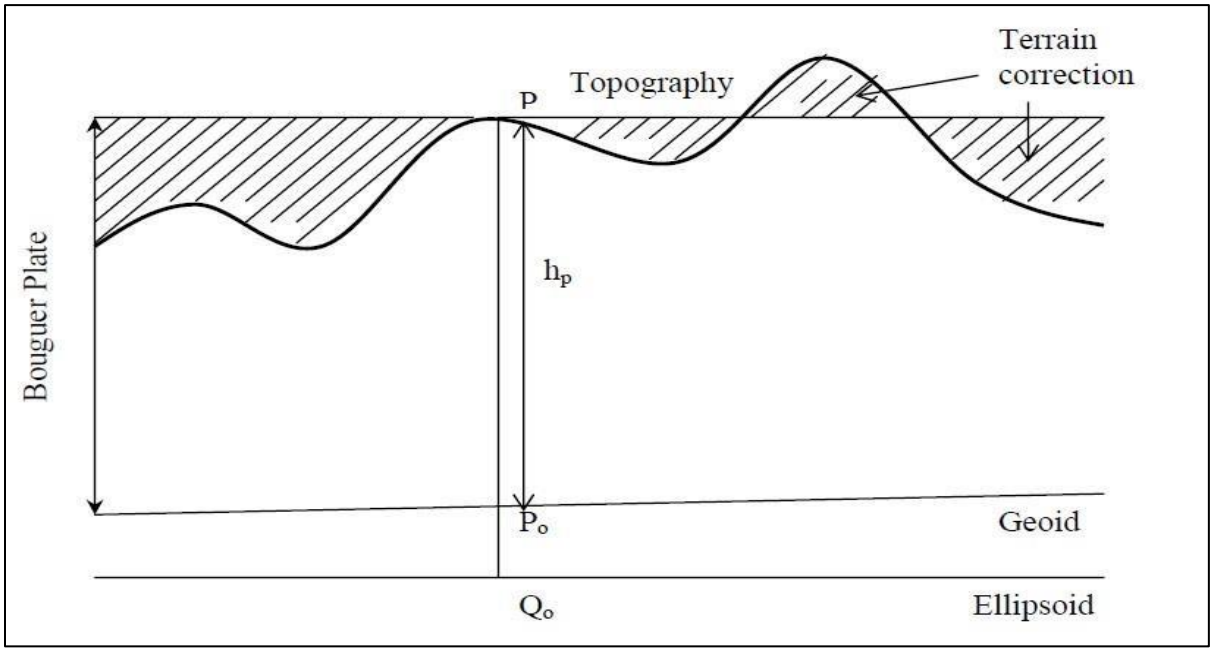

Figure 2.3: Bouguer reduction (Bajracharya, 2003)

The Bouguer plate attraction effects can be categorized into two types.

i. Incomplete Bouguer (Simple).

ii. Complete Bouguer (Refined).

Incomplete Bouguer considers only the effect due to the Bouguer plate without considering the terrain correction. That is, it ignores the topography above and below this plate. The effect of the Bouguer plate is given by Equation (2.2) (Hofmann-Wellenhof & Moritz, 2005).

$$A_B = 2\pi G\rho H \quad \text{(2.2)}$$

where,

A_B Bouguer plate effect,

G gravitational constant.

ρ crustal density

H elevation of the topography.

Complete Bouguer considers both the effect due to the bouguer plate and the terrain correction. Terrain corrections are the effects due to the deviation of the topography from the Bouguer plate (ibid). Terrain correction involves removing the masses that are above the plate and filling up the valleys below the plate. Figure (2.4) demonstrates how the masses above the plate are removed and, in the valleys, below it.

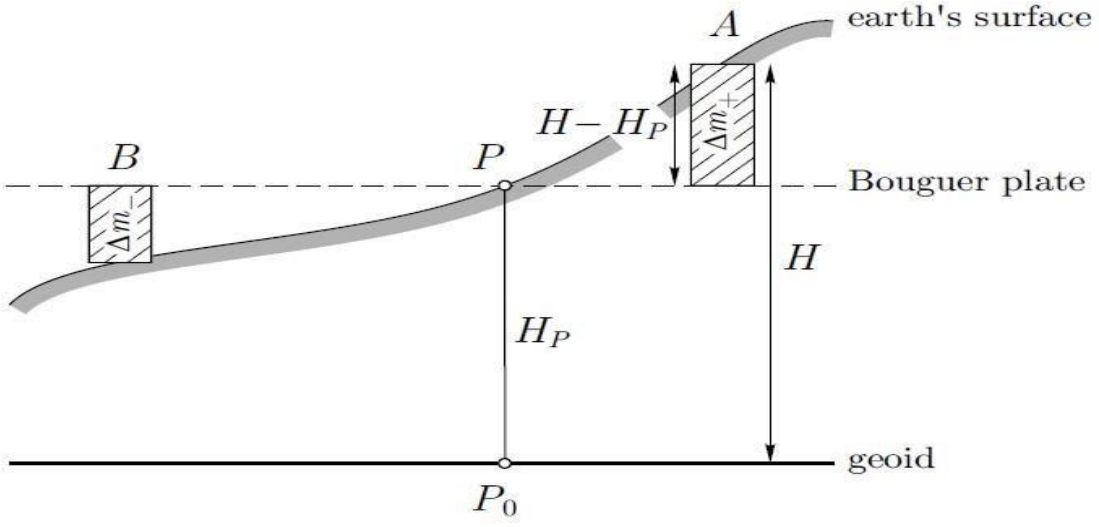

Figure 2.4: Terrain Correction (Hofmann-Wellenhof & Moritz, 2005).

Terrain correction can be computed by using equation 2.3 (Hofmann-Wellenhof & Moritz, 2005).

$$C_P = G \iiint_{h_p}^{h} \frac{\rho(x,y,z)(h_p - z)}{S^3(X_P - X, Y_P - Y, h_p - Z)} dxdydz \quad \text{(2.3)}$$

Where

C_P	terrain correction
$\rho(x, y, z)$	topographic density
h_p & h	elevations of computation and running point respectively.
G	universal gravitational constant
S	is given by Equation 2.4 below

$$S = \sqrt{(X_P - X)^2 + (Y_P - Y)^2 + (Z_P - Z)^2} \quad \text{(2.4)}$$

Where

X, Y, Z	geodetic coordinates of running points
X_P, Y_p, Z_p	geodetic coordinates of computation points.

This method can be applied in gravity smoothing for interpolation, but not for geoid determination

B. Residual Terrain Model (RTM)

Residual Terrain Model (RTM) was firstly introduced by Forsberg (1984). RTM basically provides information on the short wavelength spectral content of gravity due to topography. The information of mass distribution of the topography is presented mainly in the Digital Elevation Model (DEM). With the help of these DEM, we are able to account for the topographic masses at finer resolutions of up to 1 arc second.

After selecting a suitable DEM of the area of interest, based on either global or regional validation of DEM, the RTM method requires also to select a smooth, mean reference surface from which the DEM elevations will be referred to. This reference can either be created by averaging the DEM or through a high-order spherical harmonic expansion of the topography of earth (ibid). After selecting the reference surface, all masses that are found above this surface are removed and then filled up in the valleys below the surface (ibid) based on Equation 2.5 below. At a given range, the effect of shifting the topography will balance with the filled topography making the residual terrain effect to be small. This reduction method can be illustrated in Figure 2.5.

$$\delta A_{RTM} = G \iiint_{h_{ref}}^{h} \frac{\rho(X,Y,Z)(h_p - z)}{S^3(X_P - X, Y_P - Y, h_p - Z)} dxdydz \quad \text{(2.5)}$$

G universal gravitational constant,

h_{ref} elevation of the reference surface,

$\rho(x, y, z)$ Crustal density,

h_p Elevation of the computational point.

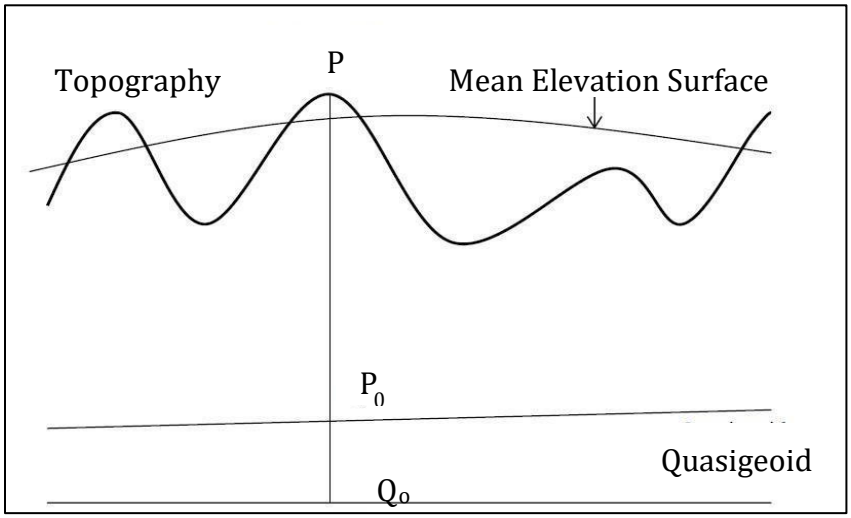

Figure 2.5: Residual Terrain Model (RTM) (Bajracharya, 2003)

This method can also be obtained by taking the difference between two separate Bouguer plates if the DEM describes well the topography (Forsberg, 1984). The first plate removes the topographic masses with a plate thickness equal to the elevation of the true topography represented by detailed elevation model and the second plate restores the topographic masses with a plate thickness equal to the elevation of the reference surface (ibid).

$$A_h = 2\pi G\rho h - C_P \quad \text{(2.6)}$$

$$A_{href} = 2\pi G\rho h_{ref} - C_P \quad \text{(2.7)}$$

where, A_h and A_{href} are the effects of Bouguer plate of the detailed elevation model and reference surface respectively, G is the Newton gravitational constant, ρ is the crustal density, h is the elevation of earth's topography as described by the detailed elevation model, h_{ref} is the elevation of the reference surface and C_P is the terrain reduction.

Taking the difference between the two plates that is equation 2.6 minus 2.7 yields equation 2.8 that describes the RTE (Forsberg, 1984).

$$\delta A_{RTM} = 2\pi G\rho(\mathrm{h} - h_{ref}) - C_P \ldots\ldots\ldots\ldots\ldots\ldots\ldots\ldots\ldots\ldots \quad (2.8)$$

where, all the symbols carry the same information as in Equation (2.6) and (2.7).

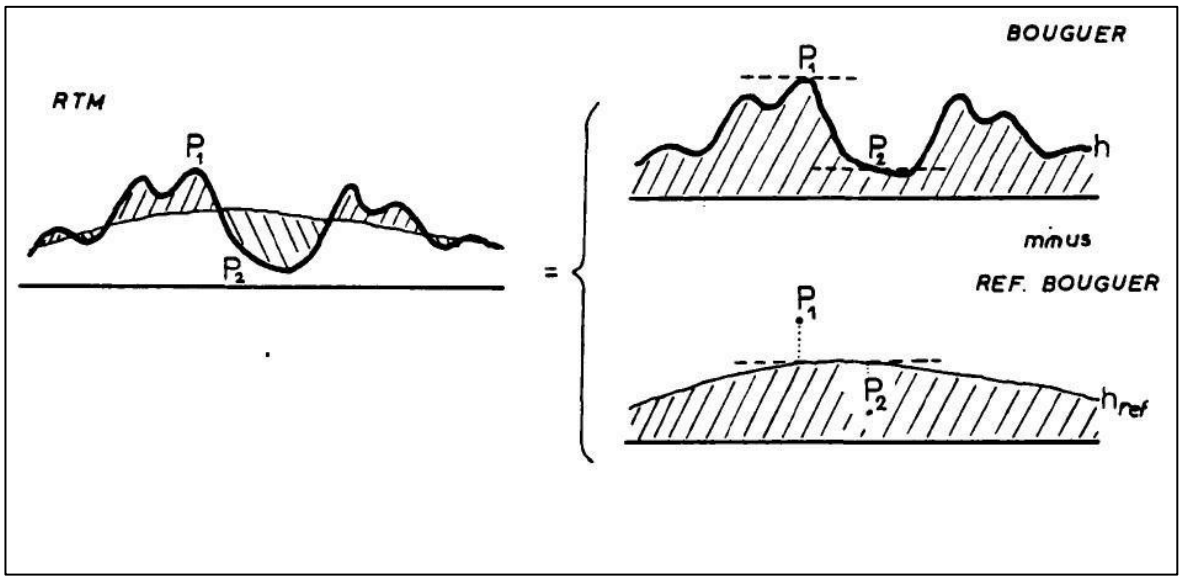

Figure 2.6: Residual terrain effects expressed as a difference of two bouguer plates represented by the topography and the reference surface (Forsberg, 1984)

This method can be applied in different physical geodesy applications that require the high frequency gravity effects such as in

i. Smoothing the actual gravity for densification and Geoid determination (Ulotu, 2009; Peter, 2018).
ii. Augmentation and validation of global Geopotential models
iii. construction of ultra-high-resolution maps of gravity field functional such as GGMplus (Hirt et al., 2013).

2.3 OVERVIEW OF GEODETIC GRAVITY FIELD MODELLING PROGRAMS

Over the past years, several geodetic gravity field modelling programs have been created to facilitate the computations of gravity field components. These programs include TC for Newton Integration

(NI) with flat-topped prism as mass elementary (Forsberg, 1984), FFT terrain correction program TCFOUR (Forsberg, 1984), POLYHEDRON for analytical computations of gravitational field of arbitrary shaped polyhedral (Tsoulis, 2012), TC Program from Gravsoft, Graflab, SRTM2gravity and TGF software (Yang et al., 2020).

2.3.1 TGF Software

Terrain Gravity Field (TGF) software is a Matlab- based program created by Yang, et al., (2020) for gravity field forward modelling of various gravity field functionals such as geoid height, gravity anomaly and all components of the gravity gradient tensors. TGF software was developed for calculating both full scale topographic and RTM gravitational field. TGF is capable of working with two both a constant density assumption and with different mass density models, and considers the curvature of the Earth by involving spherical and ellipsoidal approximations.

Generally, the topography has a complex geometric structure, which makes a general analytical solution of the Newton's integral (e.g Equation (2.4)) for any an arbitrary-shaped body impossible. For practical evaluation, numerical integration (NI) in the spatial domain technique is used (Hirt et al, 2019). This requires the topographic mass distribution to be subdivided into elementary mass elements example prisms (Forsberg & Tscherning, 2008), polyhedron (Tsoulis, 2012) or tesseroids (Grombein et al., 2013). Thereafter, the composite gravity effect is then obtained through summation of all individual gravity contribution

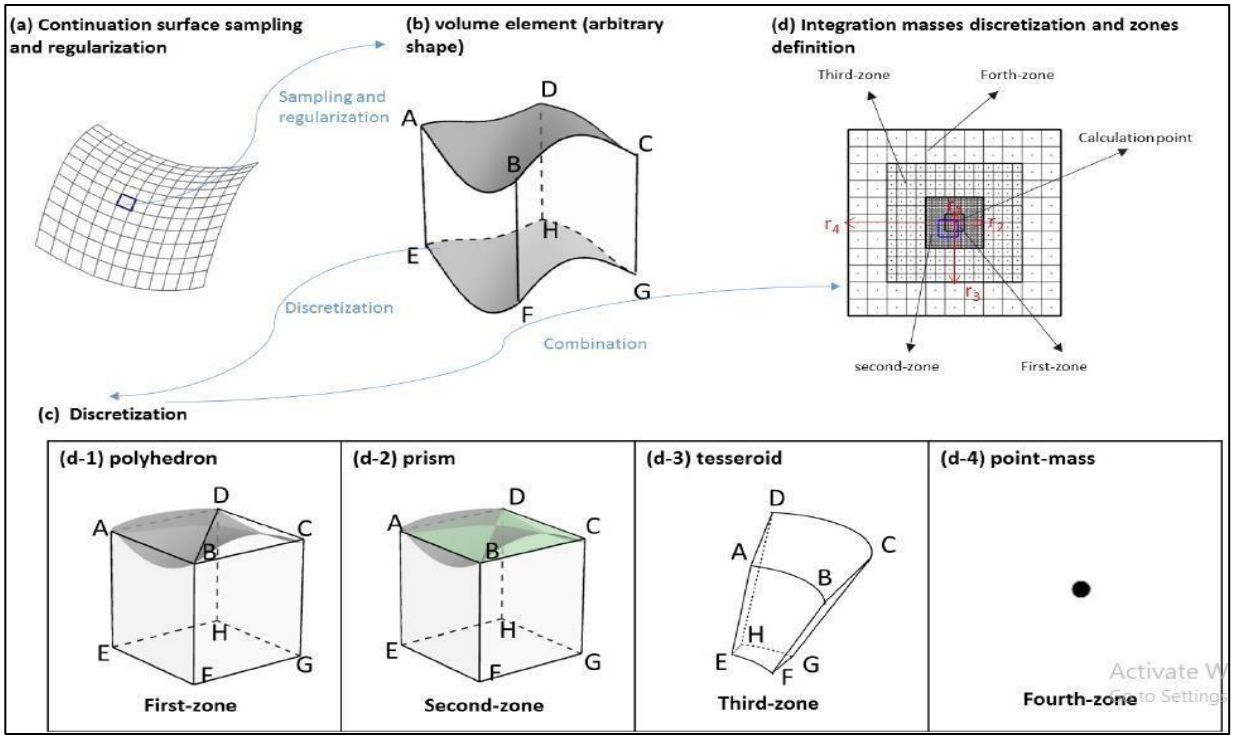

Figure 2.7: Discretization and regularization of the mass-distributions (Yang et al., 2020)

In the first zone, FORTRAN code „polyhedron" by (Toulis, 2012) is applied and combined with TGF via a so called MEX-function. For the second zone, the flat-topped prism is used for regularization as demonstrated by (Forsberg, 1984). For the third zone, tesseroids are used which are composed of three pairs of surfaces bounded by a pair of longitude, a pair of latitudes and a pair of radii as boundaries. The numerical evaluation is obtained by expanding the kernel to a third order Taylor series as demonstrated by (Grombein et al., 2013). Lastly, in the fourth zone tesseroids are replaced by point-mass of the same mass. In this method, each mass-element in the fourth zone is approximated by a point-mass. The point-mass is located in the mass-center of mass-element.

For points located inside the reference surface that is whose gravitational potential is nonharmonic, are calculated by first removing the masses above and condensing them just below the computation point. This solution is known as the harmonic correction (HC) and is given by equation (2.9) (Yang et al., 2020).

$$H_C = 4\pi G\rho H_P^{RTM} \quad \text{..... (2.9)}$$

where, H_C is the Harmonic Correction and H_P^{RTM} is the height difference between the computation point and reference surface.

Therefore, TGF software has proved to be the best compared to other gravity field modelling programs in this study since;

i. It has the ability of working with both constant density assumption and mass density models.
ii. It has the ability of working with larger datasets i.e., finer DEM resolution of 3".
iii. It combines different types of elementary mass-elements especially the more efficient tesseroid and point mass.
iv. It allows easier modification and adaptation of the MATLAB code for scientific studies.

CHAPTER THREE

METHODOLOGY.

3.1 DATA PROCESSING.

This chapter describes the methods, practical applications of the mathematical models, the data types used were explained in details, the preprocessing of these data, and the methodologies employed in the analysis.

3.1.1 Generating $1' \times 1'$ Computation Points.

The computation point file was created in surfer grid software based on the desired RTE resolution, in this case $1' \times 1'$. Computation file created was arranged in sequential form starting with computational point number (S/N), latitude(°), longitude (°), Height (m). This file was saved in .dat format and then converted to binary format (.bin), during conversion of .dat format to .bin format in Grid2bin tab the min and max lat and long are not written because in the file the min and max lat and long are indicated. Since computation points are used just to show the computing points, one DEM was used to create these points and used for all remaining DEMs. Table 3.1 below show some of computation points derived from ALOSv1-2 DEM

Table 3.1: A sample of computation point file used in computation of RTE.

S/N	Latitude (°)	Longitude (°)	Height (m)
1	-15	26.000	1088
2	-15	26.016	1078
3	-15	26.033	1085
4	-15	26.051	1090
5	-15	26.066	1091
6	-15	26.083	1115
7	-15	26.123	1139
8	-15	26.116	1165

9	-15	26.133	1211
10	-15	26.150	1188
11	-15	26.166	1212
12	-15	26.183	1220
13	-15	26.223	1220
14	-15	26.216	1218
15	-15	26.233	1203
16	-15	26.250	1211

During convention of computation points from grid format (.grd) to binary format (.bin) there are some coding lines has to be edited in the TGF Matlab software so as to enable the points to be converted perfectly. These edited coding lines are shown in the appendix I. Figure 3.1 below shows the computation points as displayed in TGF Matlab software

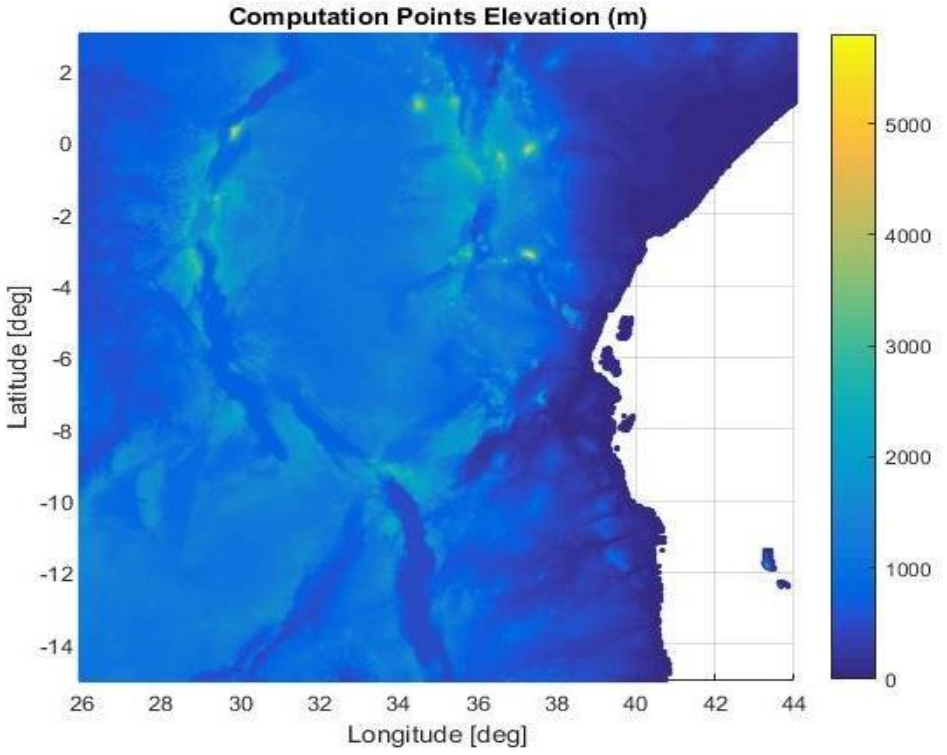

Figure 3.1: Map showing computation points as displayed in TGF Matlab software

3.1.2 Mean Reference Surface

In the computations of RTE, a smooth, long wavelength reference surface is required to be subtracted from the digital elevation model (Forsberg & Tscherning 1981). This surface as proposed by Forsberg (1894) can be constructed either by applying the moving average (MA) operator on the DEM or obtained through a high-order spherical harmonic expansion of the topography of the earth.

- **Moving Average (Ma) Reference Surface**

MA reference surface is the surface that represents the mean elevation of the area of interest for example, averaging the elevation in window to yield a mean height (Forsberg ,1984, p.37). According to (Forsberg & Tscherning, 2008) MA should be generated from DEM model of no more than spacing so as to have a reasonably smooth representation of the reference grid. The operation was carried out in Golden Surfer 15 software by passing the DEM in low-pass filter at (3x3) window. This operation was based on the same specification as in TCGRID software (Forsberg & Tscherning, 2008).

3.1.3 Generating Forward Masses.

The downloaded DEMs were gridded to produce two sets of 15 ″and 30″ resolution DEMs by using kriging method in Golden surfer software. Then, the gridded DEMs were converted to Gravsoft grid (.gri) format in Global Mapper software. Thereafter, by using grid2bin program of the TGF software, the. gri DEMs were finally converted to binary (.bin) format since TGF software accepts only binary format datasets. In the grid2bin program, the main inputs include the minimum and maximum latitude values (minlat and maxlat), the minimum and maximum longitude values (minlon and maxlon) and resolution (reslat and reslon) of the respective DEM. The respective. gri DEM to be converted was then inserted by clicking Grid file button. Figure 3.2 shows the Grid2Bin widow as displayed in TGF Matlab source code.

Figure 3.2: The grid2bin GUI for converting surfer grid to binary format

The two sets of DEMS were then among the four zones. The first and second zone shared the same DEM, which is termed as DetailedDEM in the TGF GUI software. For the third zone, the DEM was referred to as TessDEM and the fourth zone as Coarse DEM as distributed in the Table 3.2 below.

Table 3.2: Specifications of DEMs as used in TGF software in computations of RTE.

ZONE	1	2	3	4
NAME	DetailedDEM	DetailedDEM	TessDEM	CoarseDEM
GEOMETRY	polyhedron	Prism	Tesseroids	Point mass
EXTENSION (°)	0.03	0.03	0.15	0.80
RESOLUTION	15″	15″	15″	30″
FORMAT	. Bin	. Bin	. Bin	. Bin

Second, the computed reference surface was also prepared with the same procedures as the DEM. That is, the reference surfaces were gridded by using Moving average especially low pass filter of (3x3) window in Golden Surfer software to the desired resolutions. Then, the gridded reference surfaces were converted from surfer grid (.grd) format to Gravsoft (.gri) format by using Global Mapper software. The. gri formats were edited by removing the header in the Golden surfer software and make sure that the matrix is square which the main condition of TGF package is in order to perform computation otherwise cannot work and then were saved in. gri format finally converted to binary (.bin) format using grd2bin program from TGF software. The first and second zone shared the same reference surface and was referred as DetailedREF in the TGF is a GUI software. In the third zone, the reference surface was referred to as TessREF and the fourth zone as CoarseREF as summarized in the Table 3.3 below

Table 3.3: Summarizes the prepared reference surface ready for use in RTE computations in the TGF software.

ZONE	1	2	3	4
NAME	detailedREF	detailedREF	tessREF	coarseREF
RESOLUTION	15"	15"	15"	30"
FORMAT	.bin	.bin	.bin	bin

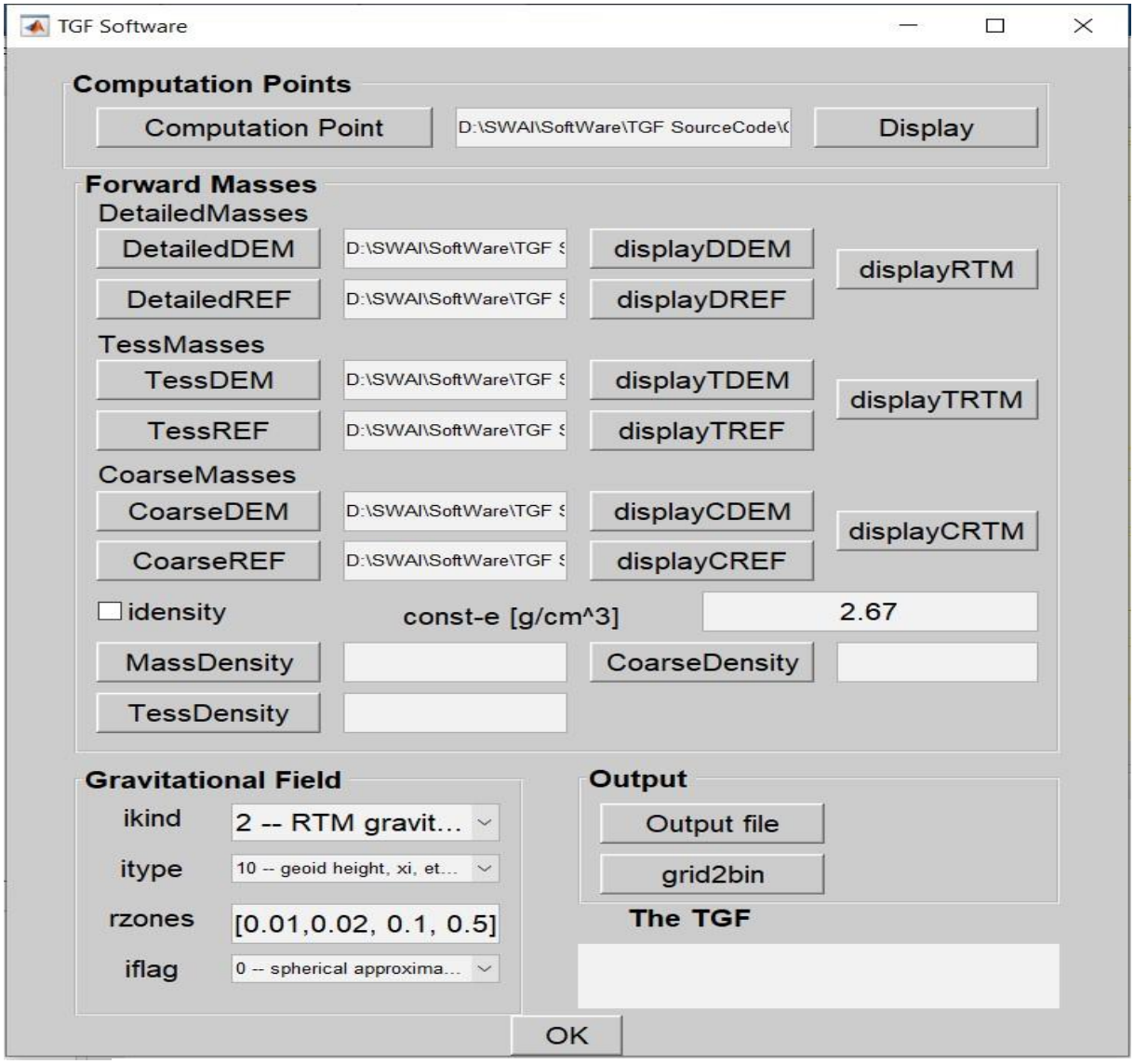

Figure 3.3: The GUI of TGF Software for the computations of RTE

Lastly, all the data were imported to The TGF software using its respective buttons as shown in Figure (3.3). Since this research computing RTE using constant density, idensity button was left unchecked. In the Gravitational Field tab, RTM gravitational field option was selected in the ikind button. Itype button that defines computation functions had the option 4 selected which computes the gravity anomaly and vertical deflections. Rzones button that defines the extension of each zone in degrees was filled with values [0.03, 0.03, 0.15, 0.8] as proposed by (Yang, et al., 2020) as the minimum requirement for attaining an accuracy of 1mGal.

3.1.4 VALIDATION OF THE RESULTS.

The critical analysis of the results is performed through statistics of the computed short -wave components of gravity (RTE) from DEMs of different resolutions which are in terms of gravity anomalies before and after finding their differences from one another within the study area via statistics including mean and standard deviation using equations presented in Table 3.4 below.

Table 3.4: Formulas for computing the statistics

S/N	Statistics	Formula
1	Difference; diff	$RTE_{\text{SRTM2Gravity}} - RTE_{\text{MERITY, TANDEM-X, FABDEM \& ALOS V1-2 DEM}}$
2	Mean; $\bar{X}$	$\frac{\sum diff}{n}$
3	Standard Deviation; STD	$\sqrt{\frac{\sum(X_i - \bar{X})^2}{n-1}}$

So far, the critical validation of the computed RTEs was done by finding the statistic of the difference between the computed RTE and the RTEs from SRTM2gravity, the static was done by finding the mean and standard deviation using Golden Surfer Software.

3.2 REQUIRED DATA

In this study, short wave components of gravity (RTE) are to be computed using TGF package in Matlab software from DEMs of different resolutions and crustal density model (a constant density). Data required are four DEMs with different resolutions which will be used in computation of RTEs and one DEM (SRTM2gravity) which will be used in the validation of the computed RTEs. The four DEMs are grouped into two in which one group is the DEMs of 1arcsec resolution (FABDEM and ALOSv1-2 DEM) and the second group is the DEMs of 3arcsec resolution (MERIT DEM and TANDEM-X). A brief description is presented below.

3.2.1 Digital Elevation Model (DEM)

In this study, DEM of different resolutions were used covering the AOI limited within 4°N to 15°S latitude and 26°E to 44°E longitude on which Tanzania is within the boundaries, (1°N to 12S° latitude and 29°E to 41°E longitude). These DEMs are MERIT DEM, ALOSv1-2 DEM , FABDEM and TANDEM-X.

- **MERIT DEM.**

Has a resolution of 3″ that is about 90m was used to provide the height information of the topography in computation of RTE. MERIT DEM file has a name that refers to interval of latitudes and longitudes of the specific area in which it covers where by only four tiles of 5°x5° were enough to cover the AOI. The horizontal and vertical datum of MERIT-3″ are WGS84 and EGM96 respectively. This model was downloaded from the website: http://hydro.iis.utokyo.ac.jp/~yamadai/MERIT_DEM .

- **FABDEM.**

Has a resolution of 1″ that is about 30m was used to provide the height information of the topography in computation of RTE. FABDEM file has a name that refers to interval of latitudes and longitudes of the specific area in which it covers where by only four tiles of 5°x5° were enough to cover the AOI. The horizontal and vertical datum of FABDEM is WGS84 and EGM08 respectively. This model was downloaded from the website https://data.bris.ac.uk/data/dataset/s5hqmjcdj8yo2ibzi9b4ew3sn

- **TANDEM-X 90m.**

TerraSAR-X add-on for Digital Elevation Measurement (TanDEM-X) is a high-resolution interferometric Synthetic Aperture Radar (SAR) mission of DLR, together with the partners EADS Astrium GmbH and Infoterra GmbH in a PPP (Public Private Partnership) consortium. The main product of the TanDEM-X mission is the TanDEM-X GDEM that contains the final GDEM of the land masses of the Earth. TanDEM-X DEM comes in 0.4^{00}, 1^{00} and 3^{00}. The 0.4^{00} & 1^{00} TanDEM-X DEMs are not made public while the 3^{00} DEM is made public. The GDEM has a horizontal resolution of 1-arc second with a coverage of the Earth's land surface from 83°N to 83°S latitude (B. Wessel, 2016). Has a resolution of 3″ that is about 90m was used to provide the height information of the topography in computation of RTE. The vertical and horizontal datum of TANDEM-X us ellipsoidal heights of WGS84. This model was downloaded from the website: https://download.geoservice.dlr.de/TDM90.

- **ALOSv1-2 DEM.**

The Advanced Land Observing Satellite (ALOS) is a Japanese earth observation satellite, developed by Japan Aerospace Exploration Agency (JAXA) formerly NASA. ALOS was developed to contribute to the fields of mapping, precise regional land coverage observation, disaster monitoring, and resource surveying. The GDEM has a horizontal resolution of 1-arc second with a coverage of the Earth's land surface from 83°N to 83°S latitude. Has a resolution of 1″ that is about 30m was used to provide height information of the topography in computation of RTE Model was downloaded in form of tiles in which each tile differs by 5°x5°.This version of ALOSv1-2 DEM dataset is provided in a WGS84 ellipsoidal vertical datum. This model was downloaded from the website: https://www.eorc.jaxa.jp/ALOS/en/aw3d30/data/index.htm.

- **SRTM2gravity.**

SRTM2gravity is a global gravity map with 3-arc second spatial resolution. It represents the gravity field implied by the Multi-Error-Removed Improved-Terrain (MERIT) DEM and a constant mass-density of 2670kgm^{-3}. The SRTM2gravity model represents the total gravitational signal of the Earth's topography in spherical approximation. The SRTM2gravity model has transformed the SRTM heights to implied gravity effects via evaluation of Newton's integral by combining spectral and spatial domain techniques for efficient and accurate computation of gravity effects (Hirt et al., 2019). The SRTM2gravity offers two data-sets namely, FullScaleGravity and ResidualGravity. The FullScaleGravity is a gravimetric terrain correction reflecting the gravitational attraction of Earth's global topography measured with respect to the geoid. It represents the linear effect of the topography on gravity, the Bouguer shell of thickness H (from DEM) together with the gravity effect of all irregularities of the topography relative to the Bouguer shell. It accounts for the total topographic effects above the geoid. The ResidualGravity is the high-frequency gravity effects reflecting the gravitational attraction of Earth's global topography residual using a reference surface of d/o 2160 SH, i.e., at scales less than 10 km (Hirt et al., 2019). 31 The SRTM2gravity data-set can be freely downloaded from the website http://ddfe.curtin.edu.au/models/SRTM2gravity2018 using a CMD code.

3.3 SOFTWARE.

Software used in this research were;

i. TGF Matlab software

This software was used in computations of RTE using constant density for both DEMs

ii. Golden Surfer software (Surfer 15)

Was used in gridding and preparations of data to be used in computation of RTE

iii. Global mapper

Was used in conversion of surfer grid and GeoTiff formats to suffer grid format.

iv. Microsoft Excel
v. Microsoft word.
vi. GMT software.

CHAPTER FOUR.

RESULTS AND ANALYSIS

4.1 RESULTS

This section presents the result attained based on the methodology and the data as described in chapter three. The results are arranged starting from the development of MA Reference Surface, computation of RTE using both DEMs and lastly validation of results.

4.1.1 DEVELOPMENT OF MA REFERENCE SURFACE

Based on the procedures described in Section 3.1.2, MA reference surface was created covering geographical location of longitude 26ºE to 44ºE and latitude 4ºE to 15ºS. The minimum elevation was -0.376m and the maximum elevation was 2096.251m. Figure 4.1 below shows the contour and surface map generated from Golden Surfer software.

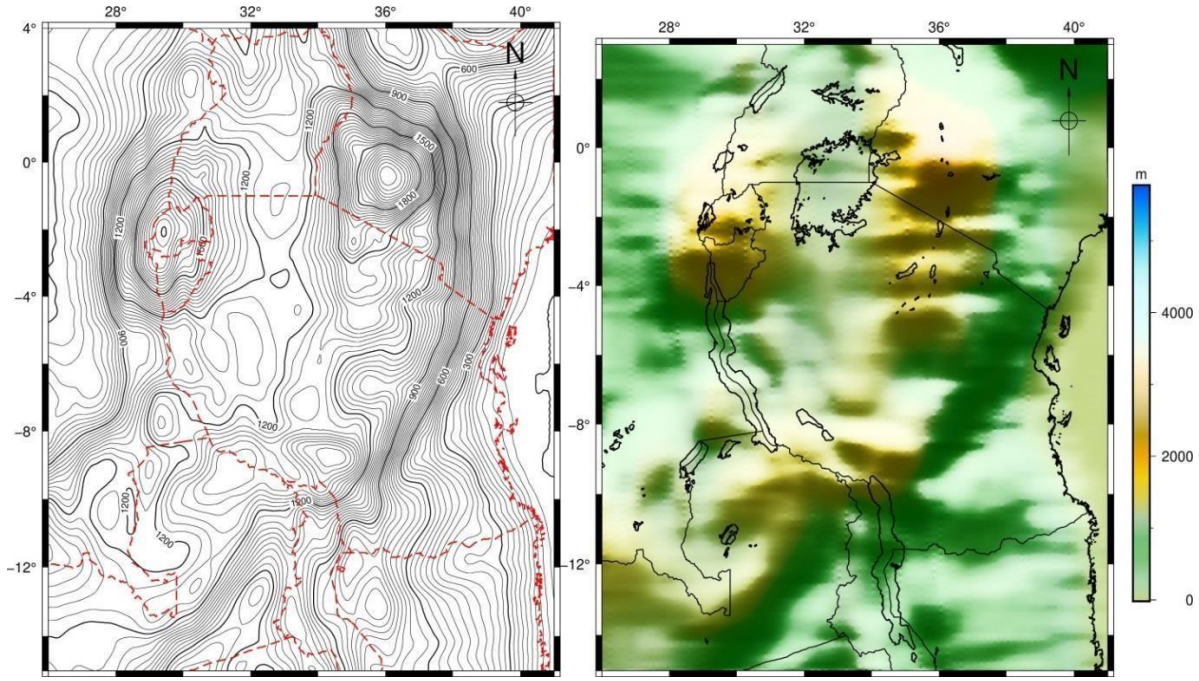

Figure 4.1: Contour and surface map of MA reference surface.

4.1.2 COMPUTED 1′ × 1′ RTE.

- **1′ × 1′ RTE from MERIT DEM.**

The 1′ × 1′ RTE was computed from MERIT DEM and the sample of results are presented in the Table 4.1 below.

Table 4.1: Sample of RTE from MERIT DEM.

LONG	LAT	RTE (mGal)
29.050	0	0.013
29.083	0	0.054
29.183	0	-0.033
29.300	0	0.035
29.3166	0	0.061
29.433	0	-0.021
29.450	0	0.124
29.466	0	-0.037
29.483	0	-0.144
30.383	0	0.046
30.400	0	-0.017
30.566	0	0.005
30.616	0	0.032
30.633	0	0.022

Table 4.2 below shows the statics of the RTEs computed from MERIT DEM using golden surfer software.

Table 4.2: Statistics of the RTE (mGal) from MERIT DEM

Minimum (mGal)	Maximum (mGal)	Mean (mGal)	95% confidence interval (mGal)	Standard deviation (mGal)
-278.932	11.366	-14.493	0.247	32.381

Figure 4.2 below shows variation of computed RTEs using MERIT DEM as plotted in GMT software. Codes used in plotting are outlined in the appendix.

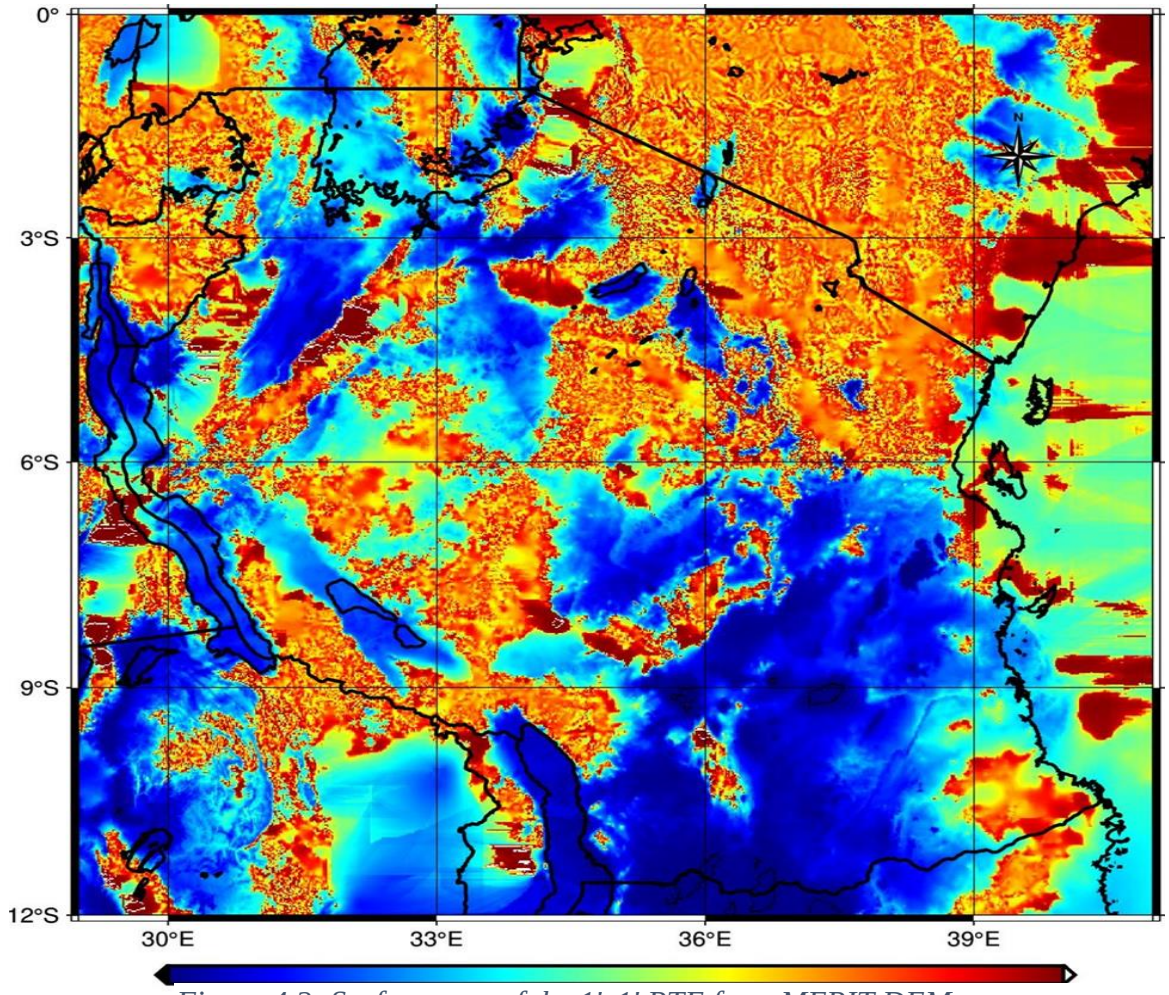

Figure 4.2: Surface map of the 1'x1' RTE from MERIT DEM

- **$1' \times 1'$ RTE from TANDEM-X.**

The $1' \times 1'$ RTE was computed from TANDEM-X and the sample of results are presented in the Table 4.3 below.

Table 4.3: Sample of RTE from TANDEM-X.

LONGITUDE	LATITUDE	RTE (mGal)
40.316	0	0.403
40.383	0	0.851
40.400	0	1.988
40.416	0	5.549
40.433	0	-0.422
29.083	-0.016	-0.919
29.183	-0.016	-0.127
29.266	-0.016	-0.893
29.333	-0.016	-0.358
29.350	-0.016	-0.444
29.366	-0.016	-0.869
29.383	-0.016	-0.499

Table 4.4 below shows the statics of the RTEs computed from TANDEM-X using golden surfer software.

Table 4.4: Statistics of the RTE (mGal) from TANDEM-X.

Minimum (mGal)	Maximum (mGal)	Mean (mGal)	95% confidence interval (mGal)	Standard deviation (mGal)
-278.945	10.553	-14.995	0.247	32.381

Figure below shows variation of computed RTEs using TANDEM-X. as plotted in GMT software. Codes used in plotting are outlined in the appendix.

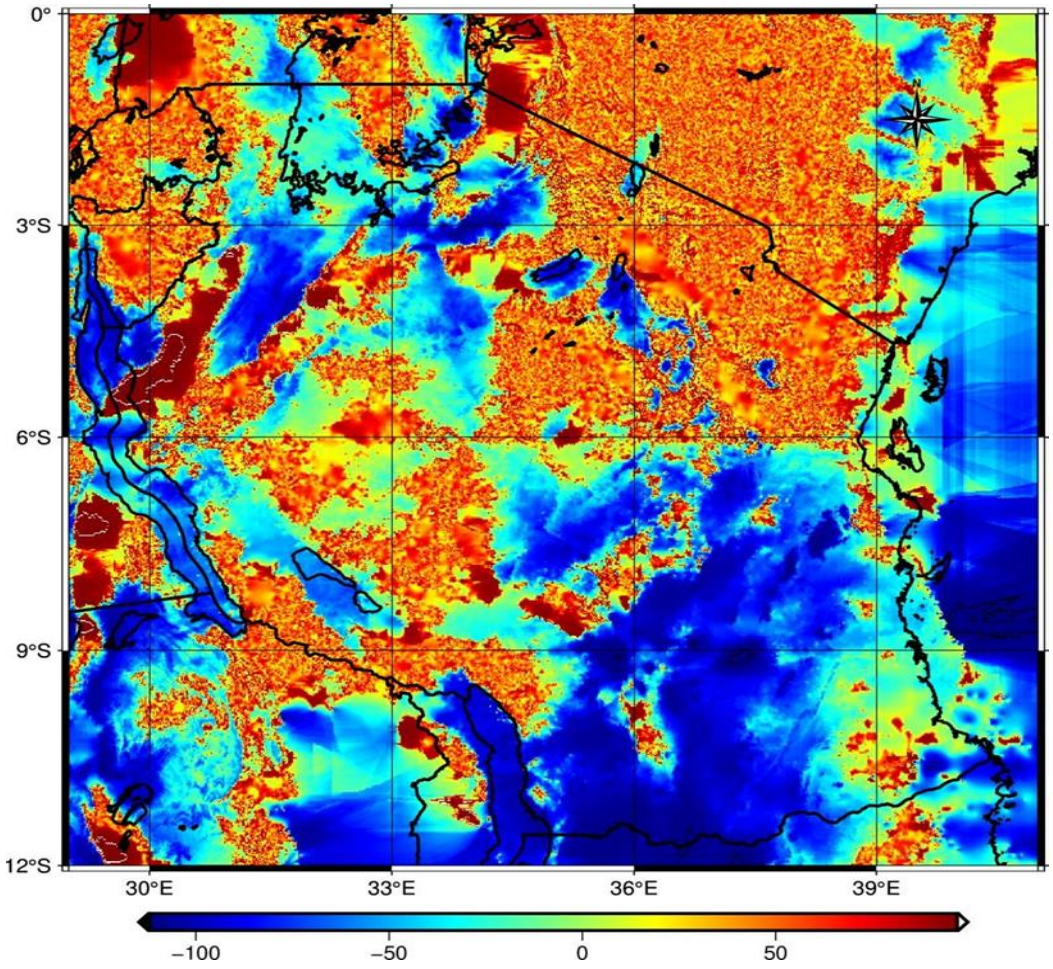

Figure 4.3: Surface map of the 1'x1' RTE from TANDEM-X

- **1′ × 1′ RTE from FABDEM**

The 1′ × 1′ RTE was computed from FABDEM and the sample of results are presented in the Table 4.5 below.

Table 4.5: Sample of RTE from FABDEM.

LONG	LAT	RTE (mGal)
40.850	-0.166	-2.549
40.866	-0.166	-2.624
40.883	-0.166	-3.388
40.900	-0.166	-2.933
40.916	-0.166	-4.194
40.933	-0.166	-5.551
40.950	-0.166	-7.317
40.966	-0.166	-8.462
40.983	-0.166	-9.603
41.000	-0.166	-9.778
29.000	-0.150	3.637
29.016	-0.150	4.370
29.033	-0.15	3.903
40.800	-0.166	-1.348

Table 4.6 below shows the statics of the RTEs computed from FABDEM using golden surfer software.

Table 4.6: Statistics of the RTE (mGal) from FABDEM

Minimum (mGal)	Maximum (mGal)	Mean (mGal)	95% confidence interval (mGal)	Standard deviation (mGal)
-115.655	20.083	-16.474	0.037	4.894

Figure 4.4 below shows variation below of computed RTEs using FABDEM as plotted in GMT software. Codes used in plotting are outlined in the appendix

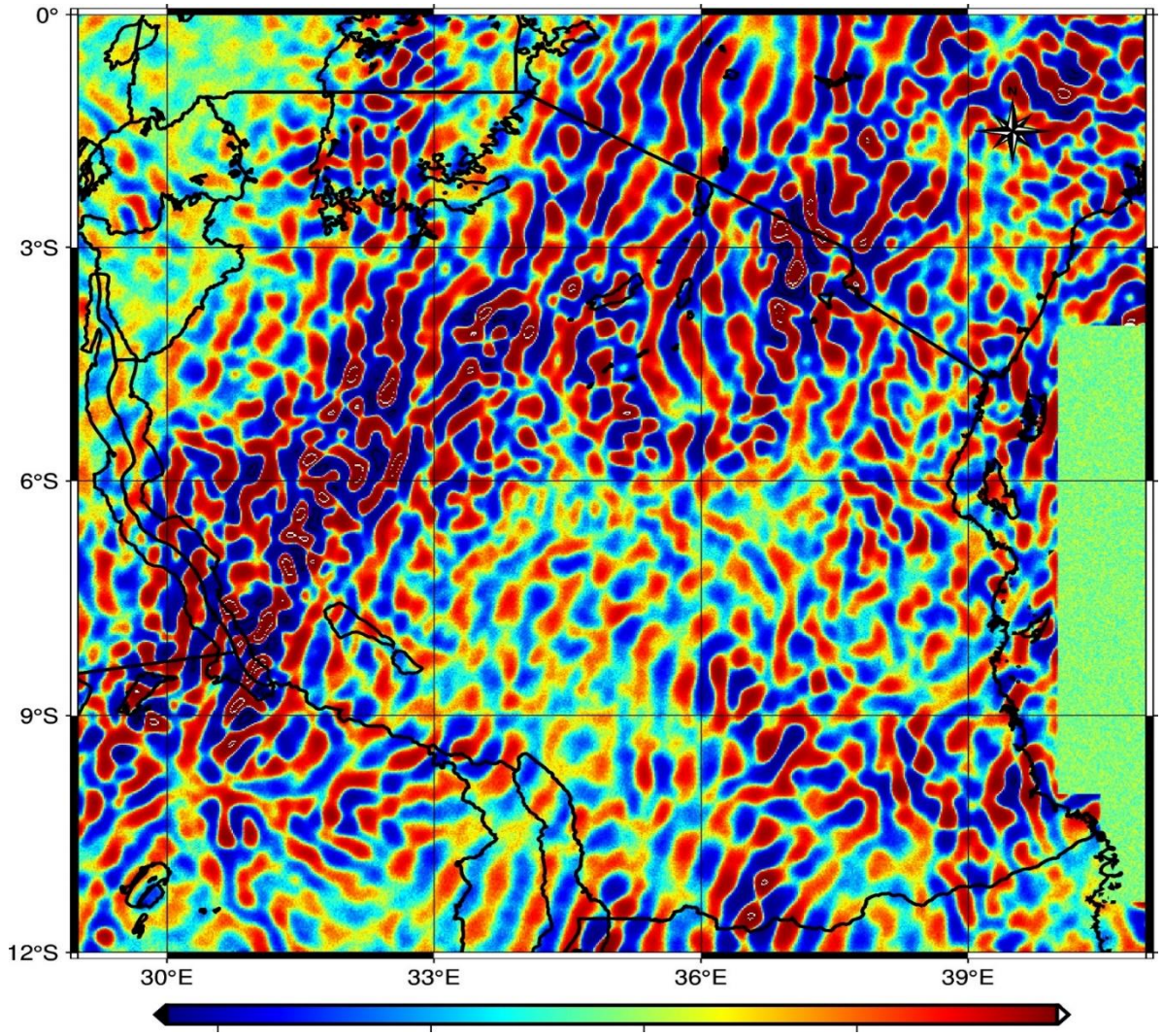

Figure 4. 4: Surface map of the 1'x1' RTE from FABDEM.

- **$1' \times 1'$ RTE from ALOSv1-2 DEM.**

The $1' \times 1'$ RTE was computed from ALOSv1-2 DEM and the sample of results are presented in the Table 4.7 below.

Table 4.7: Shows sample of RTE from ALOSv1-2 DEM.

LONG	LAT	RTE (mGal)
-11.442	28.320	-43.794
-11.441	27.816	22.167
-11.441	27.953	3.760
-11.441	28.208	-19.720
-11.441	28.026	1.992
-11.441	27.725	29.581
-11.441	28.338	-44.152
-11.440	27.797	25.664
-11.440	28.357	-47.394
-11.438	27.741	26.613
-11.438	27.778	28.250
-11.437	27.758	28.368
-11.436	27.970	3.764
-11.436	28.375	-52.603
-11.436	27.988	4.958

Table 4.8 below shows the statics of the RTEs computed from ALOSv1-2 DEM using golden surfer software.

Table 4.8: Statistics of the RTE (mGal) from ALOSv1-2 DEM

Minimum (mGal)	Maximum (mGal)	Mean (mGal)	95% confidence interval (mGal)	Standard deviation (mGal)
-149.301	29.997	-12.514	0.328	25.588

Figure 4.5 shows variation below of computed RTEs using ALOSv1-2 DEM as plotted in GMT software. Codes used in plotting are outlined in the appendix below.

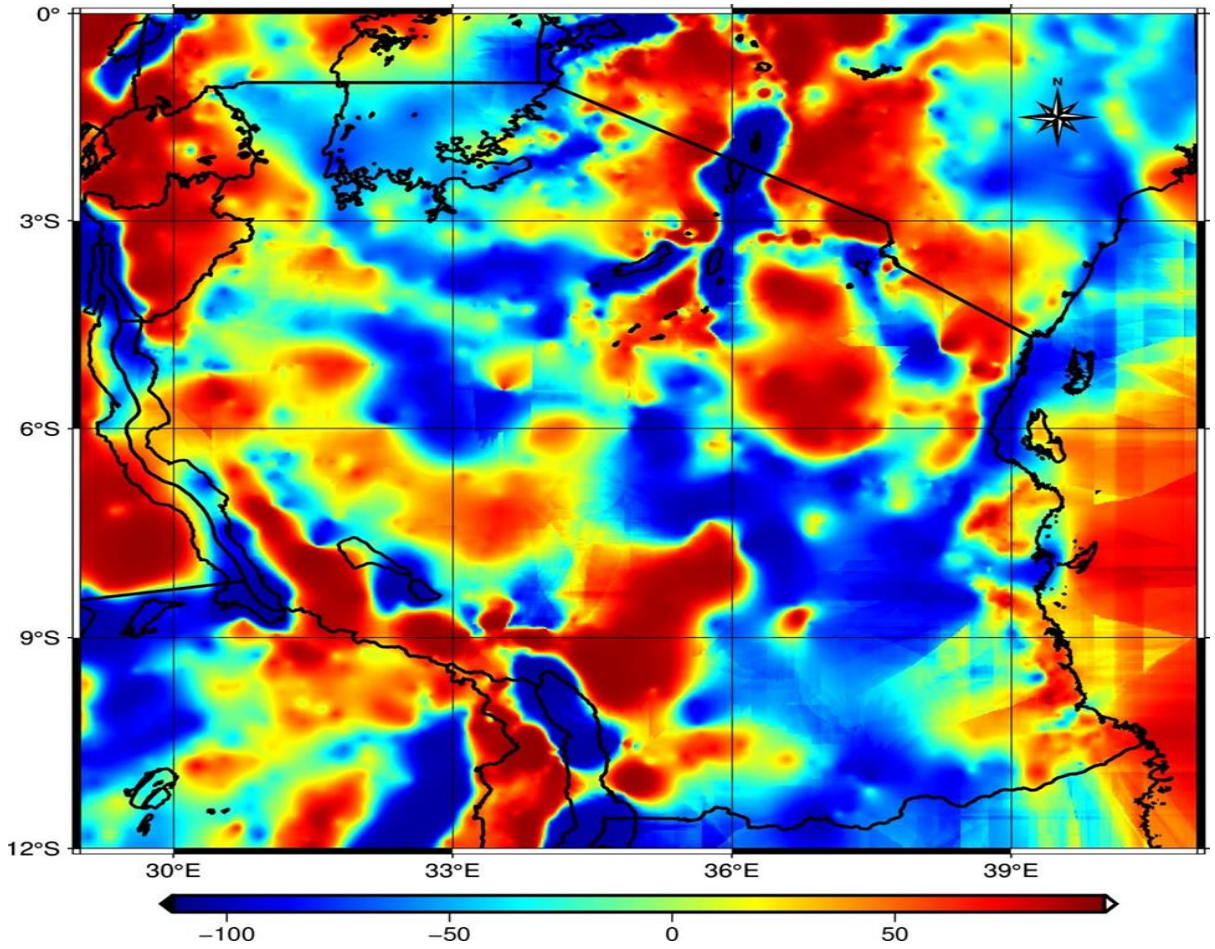

Figure 4.5: Surface map of the 1'x1' RTE from ALOSv1-2 DEM.

4.1.3 COMPARISON OF RTES

Table 4.9 below shows the statistics of RTEs computed from DEMs of different resolutions.

Table 4.9: Statistics of the computed RTE before finding their differences for both DEM.

DEM	Min (mGal)	Max (mGal)	Mean (mGal)	STD (mGal)
MERIT DEM (3arcsec)	-278.932	11.366	-14.493	32.381
TANDEM-X (3 arcsec).	-278.942	10.553	-14.995	32.381
FABDEM (1 arcsec)	-115.655	20.083	-16.474	4.894
ALOSv1-2 DEM (1 arcsec)	-149.301	29.997	-12.514	25.588

From the Table 4.9 above show that RTE computed from FABDEM are very small in terms of STD compared to other computed RTEs from other DEMs despite the fact that both are computed under the same package (TGF). This means the RTEs computed by FABDEM which is the DEM of 3arcsec are best.

Also, in order to check the computed RTE (Results) if they are the same or nearly equal or quite different need to find their differences for one to another DEMs simply because it is not enough to check the results through visualization and then by using statistical analysis especially mean and standard deviation are enough to check the results. See a brief presentation of statistics of the differences of the computed RTE from DEMs of different resolutions as tabulated below.

Table 4.10: Shows Statistics of the computed RTE finding their differences for both DEMs (MERIT, TANDEM-X, FABDEM, ALOSv1-2 DEM)

DEM	MAX	MIN	MEAN	STANDARD DEVIATION
DEMs of 1arcsec	-166.861	48.761	-7.925	17.123
DEMs of 3 arcsec	-151.608	182.399	-0.501	10.254
MERIT-FABDEM	-288.861	23.157	-17.957	32.789
MERIT-ALOS World 3D-30m DEM	-278.932	143.127	-10.032	36.492
TANDEM-FABDEM	-302.090	10.183	-31.469	32.792
TANDEM-ALOS World 3D-30m DEM	-278.942	143.105	-10.534	36.479

From the statistical Table 4.10 above show that difference of RTE computed from DEMs having the same resolutions are very small in term of mean and standard deviation compared to difference in RTE computed from DEM with different resolutions which signifies that the results obtained from DEMs of different resolutions are nearly equal.

4.2 VALIDATION OF THE COMPUTED RTES.

The results include validation of RTEs based on the SRTM2gravity data set as explained in chapter three.

4.2.1 Validation of RTEs from Merit DEM.

Table 4.11 below shows the difference of RTE obtained from RTE of MERIT DEM and RTE of SRTM2Gravity.

Table 4.11: Sample of the difference of RTE between MERIT DEM and SRTM2Gravity

LONG	LAT	RTE from SRTM2Gravity (mGal)	RTE from MERIT DEM (mGal)	Diff between SRTM2Gravity and MERIT DEM (mGal)
29.883	-12	-1.902	1.996	3.898
29.900	-12	-1.587	1.959	3.546
29.917	-12	-1.305	1.925	3.230
29.933	-12	-0.943	1.909	2.852
29.950	-12	-0.599	1.891	2.490
29.967	-12	-0.340	1.886	2.226
29.983	-12	-0.180	1.922	2.102
30.000	-12	-0.117	1.986	2.103
30.017	-12	-0.195	2.061	2.256
30.033	-12	-0.126	2.112	2.238

Table 4.12: Shows the statistical difference between MERIT DEM and SRTM2Gravity

Min (mGal)	Max. (mGal)	Mean. (mGal)	Standard Deviation. (mGal)
-46.356	278.918	14.204	32.836

4.2.2 Validation of RTEs from TANDEM-X.

Table 4.13 below shows the difference of RTE obtained from RTE of TANDEM-X and RTE of SRTM2Gravity.

Table 4.13: Sample of the difference of RTE between TANDEM-X and SRTM2Gravity

LONG	LAT	RTE from SRTM2Gravity (mGal)	RTE from TANDEM-X (mGal)	Diff between SRTM2Gravity and TANDEM-X (mGal)
29.050	0	-0.261	0.013	-0.274
29.083	0	-0.180	-0.958	0.778
29.183	0	-0.054	-0.957	0.903
29.300	0	0.011	-0.934	0.946
29.3166	0	0.027	-0.272	0.300
29.433	0	-0.074	-0.247	0.173
29.450	0	-0.209	-0.282	0.073
29.466	0	-0.171	-0.665	0.493
29.483	0	-0.290	-0.814	0.524
30.383	0	-0.550	-0.867	0.316
30.400	0	-0.130	-0.524	0.394

Table 4.14: Shows the statistical difference between TANDEM-X and SRTM2Gravity.

Max. (mGal)	Min. (mGal)	Mean. (mGal)	95% confidence level. (mGal)	Standard deviation. (mGal)
285.928	-45.815	14.705	0.251	32.830

4.2.3 Validation of RTEs from FABDEM.

Table 4.15 below shows the difference of RTE obtained from RTE of FABDEM and RTE of SRTM2Gravity.

Table 4.15: Sample of the difference of RTE between FABDEM and SRTM2Gravity.

LONG	LAT	RTE from SRTM2Gravity(mGal)	RTE from FABDEM (mGal)	Diff between SRTM2Gravity and FABDEM (mGal)
31.600	-11.983	4.686	1.644	-3.042
31.616	-11.983	5.294	1.021	-4.273
31.633	-11.983	4.310	-0.317	-4.627
31.650	-11.983	5.475	-1.748	-7.223
31.666	-11.983	4.370	-2.873	-7.244
31.683	-11.983	3.419	-3.278	-6.697
31.700	-11.983	3.765	-3.105	-6.870
31.716	-11.983	4.334	-2.296	-6.630

Table 4.16: Shows the statistical difference between FABDEM and SRTM2Gravity.

Max. (mGal)	Min. (mGal)	Mean. (mGal)	95% confidence level. (mGal)	Standard deviation. (mGal)
50.584	-55.706	-3.754	0.055	7.287

4.2.4 Validation of RTEs from Alosv1-2 Dem

Table 4.17 below shows the difference of RTE obtained from RTE of ALOSv1-2 DEM and RTE of SRTM2Gravity.

Table 4.17: Sample of the difference of RTE between ALOSv1-2 DEM and SRTM2Gravity.

LONG	LAT	RTE from SRTM2Gravity (mGal)	RTE from ALOSv1-2 DEM (mGal)	Diff between SRTM2Gravity and ALOSv1-2 DEM (mGal)
29.567	-0.017	-0.261	-20.187	19.926
29.583	-0.017	-0.180	10.496	-10.676
29.600	-0.017	-0.054	12.319	-12.373
29.617	-0.017	0.011	-34.654	34.665
29.633	-0.017	0.027	-41.658	41.686
29.650	-0.017	-0.074	-29.924	29.850
29.667	-0.017	-0.209	-19.316	19.107
29.683	-0.017	-0.171	-8.983	8.811
29.700	-0.017	-0.290	12.568	-12.858

Table 4.18: Shows the statistical difference between ALOSv1-2 DEM and SRTM2Gravity.

Max. (mGal)	Min. (mGal)	Mean. (mGal)	95% confidence level (mGal)	Standard deviation. (mGal)
173.163	-61.455	4.171	0.132	17.323

CHAPTER FIVE

CONCLUSION AND RECOMMENDATION

5.1 CONCLUSION

The main objective of this study was to assess the disparity due to use of DEMs of different resolutions in computation of RTEs. For validation results difference of RTEs between MERIT DEM and SRTM2gravity has mean of 14.204 and STD of 32.836, difference of RTEs between TANDEM-X and SRTM2gravity has mean of 14.705 and STD of 32.830, difference of RTEs between FABDEM and SRTM2gravity has mean of -3.754 and STD of 7.287 and the difference of RTEs between ALOSv1-2 DEM and SRTM2gravity has mean of 4.171 and STD of 17.323. this means FABDEM and SRTM2gravity compute the same RTE since their differences in RTEs is small in terms of mean and STD.

5.2 RECOMMENDATION

Based on the results, discussion and conclusion in this study, the following recommendations are suggested:

i. Use of a better crustal density model e.g., LITHO 1.0 in computation of RTEs from DEMs of different resolutions.
ii. Next researchers should compute RTE based on one DEM by generating other DEMs of different resolution
iii. Next researchers can predict gravity values from RTEs and used it as a cross- check with the actual gravity data.

References

Bajracharya, S. (2003). *Terrain effects on geoid determination.* MSc. Thesis,University of Calgary: Department of Geomatics Engineering, UCGE Reports Number 20181.

Bucha, B., & Janak, J. (2014). A MATLAB-based graphical user interface program for computing functionals of the geopotential up to ultra-high degrees and orders. *Efficient computations at irregular surfaces.*, .Computers & Geosciences, 66, 219-227.

Busega, H., & Kimboi, M. (2018). Surface gravity anomaly database for gravimetriv geoid model computation of Tanzania using KTH method. *A B.Sc. Dissertation of the department of Geospatial Sciences and Technology. Dar-es-Salaam: Ardhi University.*

Forsberg, R. (1984). *Updated Geoid model for Tanzania from airborne and surface gravity.*

Grombein, T., Seitz, H., & Heck. (2013). *Optimized formulas for the gravitational field of a tesseroid.* . Journal of Geodesy, 87, 645-660.

Heiskanen, & Moritz. (1967). *Physica Geodesy. W.H. Freemann and Company.* San Francisco, USA.

Hinze, W. (2003). *Hinze, W. (2003). Bouguer reduction density, .* why 2.67 Geophysics 68(5),, 1559–1560.

Hirt, C., Bucha, B., Yang, M., & Kuhn, M. (n.d.). A numerical study of residual terrain modelling (RTM) techniques and the harmonic correction using ultra-high degree spectral gravity modelling. *Journal of Geodesy*. https://doi.org/10.1007/s00190-019-01261-x

Hirt, C., Featherstone, W., & Marti, U. (2010). Combining EGM2008 and SRTM/DTM2006.0 residual terrain model data to improve quasigeoid computation in mountainous areas devoid of gravity data. *Journal of geodesy* , 84(9), 557-567.

Hofmann-Wellenhof, & Moritz. (2005). *Physical Geodesy.* Bad Vöslau, Austria: G. Grasl GmbH, 2540 Bad Vöslau, Austria.

Ince, E. S., Barthelmes, F., Reißland, S., & Elger . (2019). ICGEM: 15 years of successful collection and distribution of global gravitational models, associated services, and future plans. . *Earth Syst. Sci. Data*,, 647–674.

Kangele, T. (2021). Evaluation of XGM2019e over Tanzania using Ground gravity. *A BSc.Dissertationof the Department of Geospatial sciences and Technology, Ardhi University, Dar es salaam*.

Mai, C. (2012). *Assessment of gravity requirements for precise geoid determination in Thailand.* 33rd Asian Conference on Remote Sensing 2012. https://doi.org/ ACRS 2012.

Omang, O., & Forsberg, R. (2000). *How to handle topography in practical geoid determination: three examples.* J. Geodesy, 74, 458–466.

Peter, R. V. (2018). Tanzania Gravimetric Geoid Model (TZG17) through Quasi-Geoid by The KTH Method. *A M.Sc. Dissertation of the Department of Geospatial Sciences and Technology. Dares-Salaam: Ardhi University*.

Rexer, M., Hirt, C., & Holmes, S. (2018). *Solution to the spectral filter problem of residual terrain modelling (RTM).* J. Geodesy, 92, 675-690.

Rexer, M., Hirt, C., & Holmes, S. (2018). Solution to the spectral filter problem of residual terrain modelling (RTM). *J. Geodesy, ,* 92, 675-690.

Tziavos, I., Vergos, G., & Grigoriadis, V. (2010). *Investigation of topographic reductions and aliasing effects on gravity and the geoid over Greece based on Various digital terrain models.* Surv. Geophys, 31, 23–67.

Ulotu, P. E. (2016). *Integration of Tanzania New Gravity Network and Database into Vertical .* International Journal of Engineering Science and Computing.

Van´ıˇcek, P. ((1976)). physical geodesy lecture notes no. 43. Fredericton. *University of New Brunswick, CANADA.*

Vanicek, P., & Krakiswky, E. (1986). *Geodesy The Concept.* Elsevier Science Pub. Co.

Yang, M., Hirt, C., & Pail, R. (2020). A New MATLAB -Based Software for Terrain Related Gravity Field Calculations.

APPENDICES

GMT Codes.

a. Study area; figure 1.4

```
gmt begin out2png
1  set FONT Times-
   BoldItalic
 2
   REM Set variables for all grids
3      set
cpt1=rte1.
cpt
4      set
cpt2=rte2.
cpt
5      set
grd1=outpu
t.grd
6      set
grd2=rte1.
nc
 7


 8
   REM Make CPT for visualizing the RTE grid
9     gmt makecpt -Cjet -T0/255/1 -
H -Z > %cpt1%
10    gmt makecpt -Cjet -T-112/97 -
H -Z > %cpt2%
11


12
   REM Histogram Equalize the input grid
13 gmt grdhisteq %grd1% -
   G%grd2% -C256
14
```

```
15
  REM Convert the Histogram Equalized grid above to image
16 gmt grdimage %grd2% -C%cpt1% -JM6i -R29/41/-
  12/0 -Ba3g3
17


18
  REM Map border & Frame
19 gmt basemap -JM6i -Ba3g3 -
  R29/41/-12/0
20


21
  REM Map Coastlines
22 gmt coast -Dh -N1/1.35p -W1.25p -R29/41/-12/0 -
  Tdg39.5.0/-
23
  1.5+w1.0c+f2+l,,,N
24


25
  REM Add Color Legend
26 gmt colorbar -DJBC+w5i/0.12i+h+e -
  C%cpt2% -Ba
27


28
  REM Delete un-neccesary files
29
   Del *.nc *.cpt
3
  0
  g
  m
  t
  e
```

```
n
d
```

b. $1^0 \times 1^0$ RTE: Figure 4.2, figure 4.3, figure 4.4 and figure 4.5

```
1  gmt begin dg_rte pdf
2  REM Set variables for all grids
3  set cpt1 = rte1 . cpt
4  set cpt2 = rte2 . cpt
5  set grd1 = RTE_TZ . grd
6  set grd2 = rte1 . nc
 7
8   REM Make CPT for visualizing the RTE grid
9   gmt makecpt -Cjet -T0/255/1 -H -Z > %cpt1%
10  gmt makecpt -Cjet -T-112/97 -H -Z > %cpt2%
11
12   REM Histogram Equalize the input grid
13   gmt grdhisteq %grd1% -
G%grd2% -C256 14
15  REM Convert the Histogram Equalized grid above to image
16  gmt grdimage %grd2% -C%cpt1%
17
18  REM Map border & Frame
19  gmt psbasemap -JM4i -R%grd% -Ba
20
21  REM Map Coastlines
22  gmt coast -Dh -N1/1 .5 p -W1 .5 p
23
24  REM Add Color Legend
25  gmt colorbar -DJBC + w5i/0 .15 i + h + e -C%cpt2% -Ba -By
    + lmGal 26
27  REM Delete un-neccesary files
28  Del *. nc *. cpt
gmt end

29
```